

# Evaluating Optical Classification for *Fermi* Blazar Candidates with a Statistical method using Broadband Spectral Indices

Ting-Feng Yi<sup>1,2</sup>, Jin Zhang<sup>3,4</sup>, Rui-Jing Lu<sup>2</sup>, Rui Huang<sup>2</sup>, En-Wei Liang<sup>2,3</sup>

## ABSTRACT

We aim to test if a blazar candidate of uncertain-type (BCU) in the third *Fermi* active galactic nuclei catalog (3LAC) can be potentially classified as a BL Lac object or a flat spectrum radio quasar (FSRQ) by performing a statistical analysis of its broadband spectral properties. We find that 34% of the radio-selected BCUs (583 BCUs) are BL Lac-like and 20% of them are FSRQ-like, which maybe within 90% level of confidence. Similarly, 77.3% of the X-ray selected BCUs (176 BCUs) are evaluated as BL Lac-like and 6.8% of them may be FSRQ-like sources. And 88.7% of the BL Lac-like BCUs that have synchrotron peak frequencies available are high synchrotron peaked BL Lacs in the X-ray selected BCUs. The percentages are accordingly 62% and 7.3% in the sample of 124 optical-selected BCUs. The high ratio of source numbers of the BL Lac-like to the FSRQ-like BCUs in the X-ray and optically selected BCU samples is due to the selection effect. Examining the consistency between our evaluation and spectroscopic identification case by case with a sample of 78 radio-selected BCUs, it is found that the statistical analysis and its resulting classifications agree with the results of the optical follow-up spectroscopic observations. Our observation campaign for high- $|\rho_s|$  BCUs, i.e.,  $|\rho_s| > 0.8$ , selected with our method is ongoing.

*Subject headings:* quasars: general – BL Lacertae objects: general – gamma rays: galaxies – methods: statistical

---

<sup>1</sup>Department of Physics, Yunnan Normal University, Kunming 650500, China

<sup>2</sup>Guangxi Key Laboratory for Relativistic Astrophysics, School of Physical Science & Technology, Guangxi University, Nanning 530004, China; luruijing@gxu.edu.cn; lew@gxu.edu.cn

<sup>3</sup>National Astronomical Observatories, Chinese Academy of Sciences, Beijing 100012, China; jinzhang@bao.ac.cn

<sup>4</sup>Department of Physics and Astronomy, Purdue University, West Lafayette, IN 47907, USA

## 1. Introduction

Blazars are a particular subclass of active galactic nuclei (AGNs) with a relativistic jet toward the observers (e.g., Urry & Padovani 1995). They are divided into two groups, BL Lacertae objects (BL Lacs) and flat spectrum radio quasars (FSRQs). BL Lacs usually have no or weak emission line, while FSRQs have strong emission lines in their optical spectra. Their continuum radiations from the radio to gamma-ray ray bands are dominated by the non-thermal emission, and broadband spectral energy distributions (SEDs) are usually bimodal, which can be explained with the leptonic model (Maraschi et al. 1992; Ghisellini et al. 1996; Sikora et al. 2009; Zhang et al. 2012, 2014, 2015). In this model, the IR-optical-X-ray peak is explained as synchrotron radiation of relativistic electrons in the jets, and GeV-TeV gamma-ray bump is attributed to the inverse Compton (IC) scattering of relativistic electrons. According to the synchrotron power peak being at high (UV–soft-X-ray) or low (far-IR, near-IR) frequencies, BL Lacs are divided into high frequency peaked BL Lacs (HBLs) and low frequency peaked BL Lacs (LBLs; Padovani & Giommi 1995). Both synchrotron and IC components are presented in the soft-X-ray band in some BL Lacs, and these BL Lacs are named intermediate BL Lacs (IBLs) (Bondi et al. 2001). With the synchrotron peak frequency ( $\nu_s$ ) only, BL Lacs were assigned to low synchrotron peaked BL Lacs (LSP-BL Lacs), intermediate synchrotron peaked BL Lacs (ISP-BL Lacs), and high synchrotron peaked BL Lacs (HSP-BL Lacs), and thus this HBL–LBL subclassification changed into the classification of HSP–ISP–LSP BL Lacs in the third *Fermi*/LAT AGN catalog (3LAC). The  $\nu_s$  values of FSRQs are in the infrared and near infrared bands, being similar to that of LSP-BL Lacs (Padovani & Giommi 1995).

Gamma-ray surveys indicate that the extragalactic gamma-ray sky is dominated by blazars (Hartman et al. 1999; Abdo et al. 2010; Ackermann et al. 2011, 2015). The Energetic Gamma-Ray Experiment Telescope (EGRET) on board Compton Gamma-Ray Observatory (CGRO) discovered 66 high-confidence blazars and 27 blazar candidates among 271 sources with emission  $> 100$  MeV (the 3th EGRET Catalog; Hartman et al. 1999). The sample of gamma-ray sources is significantly enlarged by the Large Area Telescope (LAT) on board the *Fermi* satellite, which is sensitive in an energy band from 20 MeV to 300 GeV. Among 3033 gamma-ray sources in the third *Fermi*/LAT catalog (3FGL) detected between 100 MeV and 300 GeV above  $4\sigma$  significance, 1153 of the identified or associated sources are blazars, and no counterpart at other wavelengths for 1010 sources in the 3FGL (Acero et al. 2015).

Follow-up observations and association analysis with archival survey data for searching plausible radio, infrared, optical and X-ray counterparts and for revealing their emission/absorption line features of LAT sources have been performed. In the radio band, Kovalev

(2009) attempted to identify the radio counterparts by cross-correlating the gamma-ray positions with very long baseline interferometry (VLBI) positions of a large all-sky sample of extragalactic radio sources (see also Lister et al. 2011; Pushkarev & Kovalev 2012; Hovatta et al. 2014), and Ghirlanda et al. (2010) searched for associations of the sources in the first *Fermi*/LAT catalog (1FGL) with the 20 GHz Australia Telescope Compact Array (ATCA) radio survey catalog and found 230 highly probable candidate counterparts. Schinzel et al. (2015) made an all-sky radio survey for all unassociated gamma-ray sources in the second *Fermi*/LAT catalog (2FGL) to find new gamma-ray AGN associations with radio sources. They obtained firm associations for 76 previously unknown gamma-ray AGNs. Massaro et al. (2013) proposed an approach to find the radio counterparts of candidates based on the 325 MHz radio survey performed with the Westerbork Synthesis Radio Telescope and identified 23 new gamma-ray blazar candidates out of the 32 unidentified LAT sources (see also Nori et al. 2014; Giroletti et al. 2016). Petrov et al. (2013) reported their observations with the ATCA at 5 and 9 GHz of the fields around 411 unassociated LAT sources and detected 424 sources that lie within the 99 percent localization uncertainty of 283 gamma-ray sources. Lico et al. (2016) observed 84 LAT sources with the Very Long Baseline Array (VLBA) at 5 GHz and found that about 93% of these sources have a compact radio core, indicating that they should be blazar-like. In the infrared band, Massaro et al. (2011) presented a method to identify blazar candidates by examining the distributions of *Fermi* gamma-ray blazars in the three-dimensional color space defined by the IR photometry observations with the Wide-field Infrared Survey Explorer (WISE, see also D’Abrusco et al. 2012, 2013; Cowperthwaite et al. 2013; Massaro & D’Abrusco 2016). In the optical band, Massaro et al. (2014) analyzed the optical spectra available in the Sloan Digital Sky Survey data release nine (SDSS DR9) for the blazar candidates selected according to the IR color space, and found blazar-like nature of 8 out of the 27 sources. The optical spectroscopic observation campaigns were also performed to identify the blazars in the LAT gamma-ray sources (Paggi et al. 2014; Massaro et al. 2015; Landoni et al. 2015; Ricci et al. 2015; Álvarez Crespo et al. 2016a, b; Marchesini et al. 2016). By correcting archival data from literature Shaw et al. (2013a) presented spectroscopic observations covering most of the BL Lacs in the 2FGL of AGNs. Using the optical spectra of 10 *Fermi* blazars observed with the Keck telescope, Shaw et al. (2013b) also found that nine of them are BL Lacs and one is an FSRQ. In the X-ray band, Cheung et al. (2012) made X-ray follow-up observations for two bright unidentified gamma-ray sources, and Paggi et al. (2013) presented an extensive search of X-ray sources lying in the positional uncertainty regions of 205 unidentified LAT sources with available observational data obtained by the *Swift* X-ray Telescope. Masetti et al. (2013) presented optical spectroscopic observations for the putative optical counterparts of some LAT gamma-ray sources that are positionally correlated with X-ray sources observed by ROSAT, and reported that 25 out of the 30 sources are BL Lacs. Similarly, Marchesini et al. (2016) presented spectroscopic

data for 14 X-ray selected gamma-ray sources and found that 12 of them are blazars. Basing on the 3FGL and using different resources/observations in the literature, Ackermann et al. (2015) reported that among 1563 of the 2192 high-latitude ( $|b| > 10^\circ$ ) gamma-ray sources in the 3FGL are AGNs, 98% of them are blazars, but about one-third of them are blazar candidates of uncertain-type (BCUs) in 3LAC.

Distinctly statistical properties among different groups of blazars may be used to evaluate the optical classification of a BCU through analyzing its similarity to the BL Lacs and FSRQs. With the IR photometry observations by WISE it is found that blazars are distributed in a region distinct from other extragalactic sources in the IR color space (Massaro et al. 2011; D’Abrusco et al. 2012). This can be used for screening blazar candidates. Basing on that blazars show rapid flux variations on a timescale of hours in the optical band and even minutes in the high energy gamma-ray band (e.g., Gaidos et al. 1996; Mattox et al. 1997; Xie et al. 2002; Aleksić et al. 2011; Arlen et al. 2013), Chiaro et al. (2016) accessed the type of a BCU by comparing its flaring pattern in the gamma-ray band with that of BL Lacs and FSRQs. It was found that BL Lacs and FSRQs are distributed in different regions in some planes of broadband spectral indices (Padovani & Giommi 1995; Sambruna et al. 1996; Xie et al. 2003; Li et al. 2015). Padovani & Giommi (1995) showed that HBLs and LBLs are distributed in different regions in the  $\alpha_{\text{ro}}-\alpha_{\text{ox}}$  plane, where  $\alpha_{\text{ro}}$  and  $\alpha_{\text{ox}}$  are broadband spectral indices in the radio, optical, and X-ray bands. Similarly, Sambruna et al. (1996) also found that HBLs are well separated from FSRQs, while LBLs bridge the gap between the two populations (see also Ghisellini et al. 1998; Xie et al. 2003; Li et al. 2015). Ghisellini et al. (2009) showed that BL Lacs and FSRQs are well separated in the gamma-ray spectral index ( $\alpha_\gamma$ ) *vs.* gamma-ray luminosity ( $L_\gamma$ ) diagram.

This paper gives a method to evaluate the potential optical classifications of the BCUs in the 3LAC using their broadband spectral indices and gamma-ray photon indices. Note that redshift information is needed in making the  $\alpha_\gamma - L_\gamma$  diagram, but it is not for making the planes of spectral indices. Our analysis is redshift independent to evaluate the optical classifications of BCUs. We describe our samples in Section 2, and present our methodology in Section 3. Analysis results are reported in Sections 4. Comparisons with spectroscopic identifications are given in Section 5. Summary and discussion are presented in Section 6.

## 2. Sample Description

The identified 491 FSRQs and 662 BL Lacs in the 3LAC are used as a reference sample in our analysis. Among these BL Lacs, 168 sources are LSP-BL Lacs, 185 sources are ISP-BL Lacs, 286 sources are HSP-BL Lacs by adopted a criterion of  $\nu_s \leq 10^{14}$  Hz for LSP-BL Lacs,

$10^{14} < \nu_s < 10^{15}$  for ISP-BL Lacs, and  $\nu_s \geq 10^{15}$  for HSP-BL Lacs (Ackermann et al. 2015). Twenty-three BL Lacs are of unknown sub-class since no  $\nu_s$  value is available. The data of these blazars, including the  $\gamma$ -ray photon flux ( $F_\gamma$ ) and photon spectral index ( $\Gamma_\gamma$ ) in the 1–100 GeV band, the radio flux density in 1.4 or 4.8 GHz, the optical flux density in the V band<sup>1</sup>, and the X-ray flux density at 1 keV, are taken from the ASI Science Data Center (<http://www.asdc.asi.it/fermi3lac/>).

The BCU sources in the 3LAC are divided into three sub-types (Ackermann et al. 2015); BCU-Is: their optical counterparts have been identified, but the optical spectrum is inadequate to identify it as an FSRQ or a BL Lac. BCU-IIIs: their synchrotron peak frequencies can be determined from their broadband SEDs, but no optical spectra are available. BCU-IIIs: both optical spectrum and synchrotron peak frequency are not available but their broadband emission shows blazar characters with a flat radio spectrum. Among 583 BCUs<sup>2</sup> selected for our analysis 68 are BCU-Is, 429 are BCU-IIIs, and 86 are BCU-IIIs. Their data are also taken from the ASI Science Data Center (<http://www.asdc.asi.it/fermi3lac/>).

### 3. Methodology

We propose an approach to evaluate the potential classifications of these BCUs with their broadband spectral indices and gamma-ray photon spectral indices. A broadband spectral index in  $i$  and  $j$  bands is defined as,

$$\alpha_{ij} = -\frac{\log(S_i/S_j)}{\log(\nu_i/\nu_j)}, \quad (1)$$

where  $i$  and  $j$  stand for the radio (1.4 GHz), optical (V band, 5500Å), X-ray (1 keV), and  $\gamma$ -ray (1 GeV, calculated with the observed gamma-ray photon flux and index) bands, and  $S_i$  and  $S_j$  are the flux densities in the  $i$  and  $j$  bands.

The radio data are available for all blazars in the 3LAC. We calculate their  $\alpha_{r\gamma}$  values and investigate the distribution of these blazars in the  $\Gamma_\gamma - \alpha_{r\gamma}$  diagram. Since the ranges of  $\Gamma_\gamma$  and  $\alpha_{r\gamma}$  are different, i.e.,  $\Gamma_\gamma \in (1.258, 3.100)$  and  $\alpha_{r\gamma} \in (0.620, 0.916)$ , we re-scale these data in standard ranges through a linear transformation (the se-called “z-score” method)  $\tilde{z}_i = (z_i - \bar{z})/\delta_z$ , where  $\bar{z}$  and  $\delta_z$  are the mean and the standard deviation of the population  $\{z_i\}$ , respectively. This transformation ensures that 99.7% of sources ( $3\sigma_z$ ) are in the range

---

<sup>1</sup>The magnitude is converted into flux density with  $-2.5 \lg S_V = M_V - 16.44$ .

<sup>2</sup>There is 585 BCU in the 3LAC, but no radio data are available for two objects. Therefore, our BCU sample includes 583 sources.

$\tilde{z}_i \in (-3, 3)$ . The distributions of BL Lacs and FSRQs as well as their centroid points in the  $z$ -score  $\tilde{\Gamma}_\gamma - \tilde{\alpha}_{r\gamma}$  plane are shown in Figure 1(a). One can observe that FSRQs occupy the right-top corner and HSP-BL Lacs are in the left-bottom corner, and LSP-BL Lacs are mixed together with FSRQs.

We develop a method on the basis of the  $k$ -nearest neighbor (KNN) algorithm (Cover & Hart 1967; Hastie & Tibshirani 1996) evaluating a given source  $i$  to be potentially classified as a BL Lac or an FSRQ. We calculate its distances ( $r_{ij}$ ) to individual sources  $j$  of the BL Lac or the FSRQ sample in the  $z$ -score  $\tilde{\Gamma}_\gamma - \tilde{\alpha}_{r\gamma}$  plane, where  $j = 1, 2, 3, \dots, N$ , and  $N$  is the number of sources. The probability that the source  $i$  has the same type as source  $j$  is assumed to follow the second-order  $\chi^2$  distribution<sup>3</sup> of  $r_{ij}$ , i.e.,

$$p_{ij} \propto e^{-r_{ij}/2}. \quad (2)$$

We calculate  $p_{ij}$  for a given source with a reference blazar sample and scale the series  $\{p_{ij}\}$  to  $[0, 1]$  with  $p_{ij,c} = (p_{ij} - p_{ij,\min}) / (p_{ij,\max} - p_{ij,\min})$ , where  $p_{ij,\max}$  and  $p_{ij,\min}$  are the maximum and minimum values of the series. The median of  $\{p_{ij,c}\}$ , i.e.,  $p_{i,c}$ , is taken as a measurement of the statistic similarity of source  $i$  to a reference sample. A source with higher  $p_{i,c}$  indicates that it is much similar to the reference sample.

We generate a mock sample of  $10^5$  sources by randomly selecting a mimic source  $i$  in the  $\tilde{\Gamma}_\gamma - \tilde{\alpha}_{r\gamma}$  plane and calculate their  $p_{i,c}$  values to the reference samples of BL Lacs and FSRQs, i.e.,  $p_{i,c}^{\text{B}}$  and  $p_{i,c}^{\text{F}}$ , where superscripts ‘‘B’’ and ‘‘F’’ denote the BL Lac and FSRQ reference samples, respectively. The  $p_{i,c}^{\text{B}}$  and  $p_{i,c}^{\text{F}}$  contours of the mock sample are shown in Figure 1(a). It is found that the centroid points of the reference samples are within the centers of the  $p_{i,c}^{\text{B}}$  and  $p_{i,c}^{\text{F}}$  contours. From this point of view, a source that is closer to central point of a reference sample should be much similar to the reference sample. However, the mix of the  $p_{i,c}^{\text{B}}$  and  $p_{i,c}^{\text{F}}$  contours suggests that we need to jointly measure the statistic similarity of the two reference samples. We therefore define a statistic parameter as

$$\rho_{ijk} = -2 \ln(p_{ij}^{\text{F}} / p_{ik}^{\text{B}}), \quad (3)$$

where  $j = 1, \dots, N^{\text{F}}$ ,  $k = 1, \dots, N^{\text{B}}$ ,  $N^{\text{F}}$  and  $N^{\text{B}}$  are the numbers of the reference BL Lacs and FSRQs, respectively. The definition is similar to the statistic test used in Mattox et al. (1996) for measuring the likelihood of source detection, in which they determined the

---

<sup>3</sup>By simply using the distance to measure the probability, we can also get similar results. However, by adopting that the probability as a function of the distance follows the second-order  $\chi^2$  distribution, the classification of two types of blazars is significantly improved, especially for those HSP-BL Lacs and FSRQs in the left-bottom and right-top corners.

detection significance of a gamma-ray source with likelihood ratio  $T_s \equiv -2 \ln L_0/L_1$ , where  $L_0$  is the likelihood of the null hypothesis that no point source exists at the position under consideration and  $L_1$  is the likelihood of the converse hypothesis.

We take the median value of a series  $\{\rho_{ijk}\}$  as the test statistic for the given source  $i$ , i.e.,  $\rho_{i,c}$ . We scale  $\{\rho_{i,c}\}$  into  $\{\rho_{i,s}\}$  with a linear function of  $\rho_{i,s} = -1 + 2 \times (\rho_{i,c} - \rho_{i,c,\min})/(\rho_{i,c,\max} - \rho_{i,c,\min})$ , where  $\rho_{i,c,\max}$  and  $\rho_{i,c,\min}$  are the maximum and minimum values of series  $\{\rho_{i,c}\}$ . The scaled set of  $\{\rho_{i,s}\}$  then is in the range of  $[-1, 1]$ . Noting that one can also scale  $\{\rho_{i,s}\}$  values into  $[0, 1]$  with  $\rho_{i,s} = (\rho_{i,c} - \rho_{i,c,\min})/(\rho_{i,c,\max} - \rho_{i,c,\min})$  to reflect the hypothesis that a given source belongs to or not a group. We here re-scale  $\{\rho_{i,s}\}$  values into  $[-1, 1]$ . The re-scaled  $\{\rho_{i,s}\}$  is taken as a statistical parameter to evaluate the potential optical classification of a source. With our definition, a source with  $\rho_s > 0$  is similar to the BL Lac, otherwise it is likely an FSRQ. Figure 1(b) shows the contours of  $\rho_s$  for the mock reference sample of  $10^5$  sources. One can observe that the contours are hyperbolic-like curves, but not closed ellipses.

Optical and X-ray data are also available for some BL Lacs and FSRQs in our reference samples. Figure 2 shows the distributions of these BL Lacs and FSRQs in the  $z$ -score spectral planes, where the spectral indices are defined with different sets of  $\{\alpha_{ij}, \alpha_{kl}\}$  and  $\{\alpha_{ij}, \Gamma_\gamma\}$ , where  $i, j, k, l \in \{r, o, x, \gamma\}$ ,  $i \neq j$ , and  $k \neq l$ . One can observe that the two kinds of blazars are roughly separated in these planes, being similar to that shown in Figure 1, except for the planes of  $\tilde{\alpha}_{ox} - \tilde{\alpha}_{o\gamma}$ ,  $\tilde{\alpha}_{ox} - \tilde{\alpha}_{x\gamma}$ , and  $\tilde{\alpha}_{o\gamma} - \tilde{\alpha}_{x\gamma}$ , in which two kinds of blazars are mixed together. We calculate the  $\rho_s$  values for the mock sample and show the  $\rho_s$  contours in Figure 2.

Inspecting the distributions of the sub-classes of BL Lacs in these spectral planes, it is found that HSP-BL Lacs are well separated from FSRQs, ISP-BL Lacs fill the gap between HSP-BL Lacs and FSRQs, and LSP-BL Lacs are merged into the region of FSRQs. We remove both ISP-BL Lacs and LSP-BL Lacs from Figure 2 and derive the  $\rho_s$  contours for the HSP-BL Lacs and FSRQs only. They are shown in Figure 3. It can be seen that most of them are separated with a division line at  $\rho_s \sim 0$ , except for the three spectral planes mentioned above, i.e.,  $\tilde{\alpha}_{ox} - \tilde{\alpha}_{o\gamma}$ ,  $\tilde{\alpha}_{ox} - \tilde{\alpha}_{x\gamma}$ , and  $\tilde{\alpha}_{o\gamma} - \tilde{\alpha}_{x\gamma}$ .

Noting that most spectral planes shown in Figures 2 and 3 are not intrinsically independent since they are derived by crossly using the gamma-ray, X-ray, optical, and radio data. According to the results above and the data available for the BCU sample, we select the spectral planes of  $\tilde{\Gamma}_\gamma - \tilde{\alpha}_{r\gamma}$ ,  $\tilde{\Gamma}_\gamma - \tilde{\alpha}_{rx}$ , and  $\tilde{\alpha}_{ox} - \tilde{\alpha}_{r\gamma}$  for evaluating the potential classification of the BCUs in the 3LAC. The  $\tilde{\Gamma}_\gamma - \tilde{\alpha}_{r\gamma}$  plane uses only the gamma-ray and radio data. The X-ray and optical data are used in the  $\tilde{\Gamma}_\gamma - \tilde{\alpha}_{rx}$  and  $\tilde{\alpha}_{ox} - \tilde{\alpha}_{r\gamma}$  planes.

With a criterion of  $\rho_s = 0$  one may statistically recognize a given source as a BL Lac or an FSRQ on the basis of our definition of  $\rho_s$ . However, the confidence level ( $\sigma$ ) of such a judgement with different spectral planes is different. The left panels of Figure 4 show  $\sigma$  as a function of  $\rho_s$  for the BL Lacs and FSRQs in the three spectral planes. The cumulative probabilities ( $P$ ) as a function of  $\rho_s$  are also shown in the left panels of Figure 4. We calculate the confidence lever for evaluating a source with  $\rho_s$  to be a BL Lac by

$$\sigma^{\text{B}}(\rho_s) = \frac{N^{\text{B}} * [1 - P^{\text{B}}(\rho_s)]}{N^{\text{B}} * [1 - P^{\text{B}}(\rho_s)] + N^{\text{F}} * P^{\text{F}}(\rho_s)} \times 100\%, \quad (4)$$

which is the percentage of the BL Lacs in the global sample in the range of  $> \rho_s$ . Accordingly,  $\sigma^{\text{F}}(\rho_s)$  is given by  $\sigma^{\text{F}}(\rho_s) = 1 - \sigma^{\text{B}}(\rho_s)$ . The cross points “A” shown in the left panels of Figure 4 are for  $\sigma^{\text{F}}(\rho_s) = \sigma^{\text{B}}(\rho_s) = 50\%$ .

By adopting  $\sigma > 90\%$ , the corresponding  $\rho_s$  for the BL Lacs and the FSRQs in the  $\tilde{\Gamma}_\gamma - \tilde{\alpha}_{\text{r}\gamma}$  plane are  $\rho_s > 0.35$  and  $\rho_s < -0.60$ , respectively. It is found that 59% of the BL Lacs and 49% of the FSRQs are in the range of  $\rho_s > 0.35$  and  $\rho_s < -0.60$ . Similarly, for  $\sigma > 90\%$ , 84% of the BL Lacs are in the range of  $\rho_s > -0.18$  and 59% of the FSRQs are of  $\rho_s < -0.70$  in the  $\tilde{\Gamma}_\gamma - \tilde{\alpha}_{\text{r}\text{x}}$  plane, and 70% of the BL Lacs are in the range of  $\rho_s > 0.20$  and 50% of the FSRQs are in the range of  $\rho_s < -0.60$  in the  $\tilde{\alpha}_{\text{ox}} - \tilde{\alpha}_{\text{r}\gamma}$  plane. These results are illustrated with the points of “B” and “C” and the shaded regions in the left panels of Figure 4. The X-axis values of the “B” and “C” points correspond to the  $\rho_s$  values of  $\sigma = 90\%$  for the selected BL Lac and FSRQ samples, and their Y-axis values are the cumulative probabilities at the corresponding  $\rho_s$  values. The shaded regions thus mark the percentages of sources that are statistically analogue to the selected BL Lac or FSRQ samples within  $\sigma > 90\%$ .

#### 4. Analysis Results for BCUs

The  $\rho_s$  contours shown above present a statistical similarity for a given source in these planes to the blazar samples. In this section, we derive the  $\rho_s$  values for the BCUs in the 3LAC.

Radio data are available for all BCUs in our sample (radio-selected BCUs). We calculate their  $\alpha_{\text{r}\gamma}$  values, which are reported in Table 1. We examine whether the distribution of these BCUs in the  $\Gamma_\gamma - \alpha_{\text{r}\gamma}$  plane is statistically consistent with the blazar sample by utilizing the two-dimensional Kolmogorov–Smirnov test (K–S test)<sup>4</sup>. We obtain  $p_{\text{KS}} = 0.017$ , marginally

---

<sup>4</sup>The K–S test yields a chance probability of  $p_{\text{KS}}$ . A two-dimensional K–S test probability ( $p_{\text{KS}}$ ) larger



suggesting that the two samples are from the same parent population.

We calculate the  $\rho_s$  values of these BCUs. Our results are also reported in Table 1. The top-right panel of Figure 4 shows the distribution of the radio-selected BCUs in the  $\tilde{\Gamma}_\gamma - \tilde{\alpha}_{r\gamma}$  plane, together with the contours of  $\rho_s$  derived from the identified BL Lacs and FSRQs (reference samples). Adopting  $\rho_s > 0.35$  and  $\rho_s < -0.60$  as derived from the BL Lacs and FSRQs, we find that 201 and 114 out of the 583 radio-selected BCUs are potentially classified as BL Lacs and FSRQs within  $\sigma > 90\%$ .

Radio and X-ray data are available for 176 BCUs (X-selected BCUs), and among them 124 BCUs (optical-selected BCUs) also have optical data available. We calculate their broad-band spectral indices ( $\alpha_{rx}$ ,  $\alpha_{r\gamma}$  and  $\alpha_{ox}$ ) and the  $\rho_s$  values in the  $\tilde{\Gamma}_\gamma - \tilde{\alpha}_{rx}$  and  $\tilde{\alpha}_{ox} - \tilde{\alpha}_{r\gamma}$  planes. Our results are also reported in Table 1. Their distributions in the  $\tilde{\Gamma}_\gamma - \tilde{\alpha}_{rx}$  and  $\tilde{\alpha}_{ox} - \tilde{\alpha}_{r\gamma}$  planes together with the contours of  $\rho_s$  derived from the reference sample are shown in the right panels of Figure 4. We find that among 176 X-selected BCUs, 77.3% (136 sources) are similar to the BL Lacs with  $\rho_s > -0.18$ , and 6.8% (12 sources) are analogue to the FSRQs with  $\rho_s < -0.70$  within  $\sigma > 90\%$ . Among the optical-selected BCUs, 62% (77/124) of sources statistically resemble to the BL Lac type with  $\rho_s > 0.20$  and 7.3% (9 sources) would be FSRQ-like within  $\sigma > 90\%$ . The high ratio of the BL Lac-like to the FSRQ-like BCUs in the X-ray and optically selected BCU samples is due to the selection effect. For example, Masetti et al. (2013) performed the optical spectroscopic observations for a sample of 30 X-ray selected LAT gamma-ray sources and found that 25 of them are BL Lac-type. Our results are summarized in Table 2. The optical classifications of those BCUs that lay in the regions out of the  $\rho_s$  contours for  $\sigma(\rho_s) < 90\%$  are uncertain with our criteria.

As shown in Figure 3, HSP-BL Lacs are usually well separated from FSRQs. We show the distribution of  $\rho_s$  and  $\rho_s$  as a function of  $\log \nu_s$  for the X-selected BCUs in Figure 5. A source with higher  $\nu_s$  tends to have a larger  $\rho_s$  value. Comparisons of the  $\nu_s$  distributions between the BCUs that are statistically similar to the BL Lacs and FSRQs within  $\sigma > 90\%$  with the different groups of blazars in the reference sample are also given in Figure 5. One can observe that the  $\nu_s$  distribution of the BL Lac-like BCUs is similar to that of HSP-BL Lacs in the reference sample, and 88.7% of BL Lac-like BCUs (102/115) that have  $\nu_s$  available are HSP-BL Lac-like.

---

than 0.1 would strongly suggest no statistical difference between two samples, and the hypothesis that the two samples are from the same parent population is rejected with a confidence level larger than  $3\sigma$  with  $p_{KS} < 10^{-4}$ .

## 5. Comparisons with Spectroscopic Identifications

Any statistical approach cannot give the conclusive optical type of a BCU. To examine the consistency of our results with identification of spectroscopic observations, we compare our analysis results with that of the spectroscopic campaigns reported in Massaro et al. (2016). 78 radio-selected BCUs in the 3LAC have been identified as BL Lac-type (63 sources) and FSRQ-type (15 sources) by Massaro et al. (2016, reference therein), and 34 sources out of them are in our X-selected sample and 28 sources out of them are in our optical-selected sample. Figure 6 and Table 3 show the comparison case by case. It is found that 42 out of the 63 BL Lacs are evaluated as BL Lac-like and one source is mistaken as FSRQ-like within  $\sigma > 90\%$  with our method. Among the 15 FSRQs, 9 are assigned as FSRQ-like and only one source is mistaken as BL Lac-like. For the 34 X-selected BCUs, 31 are identified as BL Lacs by Massaro et al. (2016), and 29 of them are suggested to be BL Lac-like and none of them is mistaken as FSRQ-like with our method within  $\sigma > 90\%$ . Three out of the 34 X-selected BCUs are identified as FSRQs by Massaro et al. (2016), only one case can be picked up with our method. Similar results are also found in the 28 optical-selected BCUs.

## 6. Summary and Discussion

Utilizing the BL Lacs and FSRQs in the 3LAC as templates, we have developed a statistical method to evaluate the potential optical classification of the BCUs in 3LAC with their spectral indices in the gamma-ray, X-ray, optical, and radio bands. Our results are summarized as followings.

- 34% and 20% of 583 radio-selected BCUs are BL Lac-like and FSRQ-like sources, respectively, and 46% of the BCUs cannot be claimed as BL Lac-like or FSRQ-like within  $\sigma > 90\%$  with our method. The ratio of source numbers of the BL Lac-like to the FSRQ-like BCUs is 1.7, which is larger than that of the reference sample (1.35) with a factor of 1.26.
- 77.3% and 6.8% of the 176 X-selected BCUs are BL Lac-like and FSRQ-like sources, respectively, and about 16% of the X-selected BCUs cannot be claimed as BL Lac-like or FSRQ-like within  $\sigma > 90\%$  with our method. Similarly, the percentages of the BL Lac-like and FSRQ-like objects in the 124 optical-selected BCUs are 62% and 7.3%, respectively. The high ratio of source numbers for the BL Lac-like to the FSRQ-like BCUs in the X- and optical-selected BCUs is due to the sample selection effect.
- HSP-BL Lac-like BCUs are more efficiently selected than ISP/LSP-BL Lac-like BCUs

since ISP/LSP-BL Lacs are analogue to FSRQs with our method. 102 sources out of the 115 BL Lac-like BCUs that have the  $\nu_s$  values available are HSP-BL Lac-like objects.

- We examined the consistency between our analysis results with spectroscopic identification case by case using a radio-selected sample of 78 BCUs (63 BL Lacs and 15 FSRQs) from Massaro et al. (2016). It shows that 67% of the BL Lacs and 60% of the FSRQs in this sample can be correctly picked up within  $\sigma > 90\%$  and only one BL Lac and one FSRQ are mistaken as a wrong type with our method. Thirty-four out of the 78 BCUs also have the X-ray data available. Thirty-one of them were identified as BL Lacs by Massaro et al. (2016), among which 29 sources are suggested to be BL Lac-like within  $\sigma > 90\%$  with our method.

Our method evaluate a BCU to be potentially classified as a BL Lac or a FSRQ with its position in the selected planes defined by the broadband spectral indices. Selection effects of the different detection thresholds and energy bands in instruments may affect the source distributions in these spectral planes, hence affect the analysis results of this work. From the lower panel of Figure 1, one can observe that the derived contours of  $\rho_s$  are hyperbolic-like curves. Extreme BL Lacs and FSRQs with the large  $|\rho_s|$  values, such as  $|\rho_s| > 0.8$ , are in the left-bottom corner (for BL Lacs) or right-top corner (for FSRQs). No blazar is populated into the left-top and right-bottom corners. Noting that the analysis for sources in these regions with our priori estimator may take a great risk if the lack of sources in this regions is due to observational selection effects. However, this would not be due to the observational selection effects, but is lack of blazars with such kind of spectral properties. It was found that gamma-ray flux of blazar in the LAT band is positively corrected with the radio flux density (e.g., Ghirlanda et al. 2011). Sources in the left-top or right-bottom corner with a large  $\alpha_{r\gamma}$  (corresponding to a high radio flux and a low gamma-ray flux) or a small  $\alpha_{r\gamma}$  (corresponding to a low radio flux and a high gamma-ray flux) would violate this positive correlation.

Although analysis with our method cannot give a conclusive type to a BCU, it may be helpful for source selection in the spectroscopic observation campaigns and for population statistical analysis. On the basis of our analysis, we currently perform a spectroscopic and photometric campaign with the 2.4 m and 2.16 m telescopes in Lijiang and Xinlong Observatories for the BCUs with larger  $|\rho_s|$  value, i.e.,  $|\rho_s| > 0.8$  from the radio-selected BCU sample. Our purpose is not only to confirm types of these BCUs, but also try to find new TeV blazar candidate for the coming TeV surveys with the Cherenkov Telescope Array (CTA) and Large High Altitude Air Shower Observatory (LHASSO, Costamante 2007; Zhao et al. 2016).

## Acknowledgements

We thank the anonymous referee for his/her valuable suggestions. This work is based on the published data from the ASI Science Data Center (ASDC). This work is supported by the National Basic Research Program (973 Programme) of China (grant 2014CB845800), the National Natural Science Foundation of China (grants 11533003; 11463001, 11573034, 11263006, 11363002, 11322328, 11373036), the joint fund of Astronomy of the National Nature Science Foundation of China and the Chinese Academy of Science (grant U1431123), Yunnan province education department project (grant 2014Y138), and the Guangxi Science Foundation (2013GXNSFFA019001, 2014GXNSFAA118011).

## REFERENCES

- Abdo, A. A., Ackermann, M., Ajello, M., et al. 2010, *ApJ*, 715, 429
- Acerro, F., Ackermann, M., Ajello, M., et al. 2015, *ApJS*, 218, 23
- Ackermann, M., Ajello, M., Allafort, A., et al. 2011, *ApJ*, 743, 171
- Ackermann, M., Ajello, M., Atwood, W. B., et al. 2015, *ApJ*, 810, 14
- Aleksić, J., Antonelli, L. A., Antoranz, P., et al. 2011, *ApJ*, 730, L8
- Álvarez Crespo, N., Masetti, N., Ricci, F., et al. 2016a, *AJ*, 151, 32
- Álvarez Crespo, N., Massaro, F., Milisavljevic, D., et al. 2016b, *AJ*, 151, 95
- Bondi, M., Marchã, M. J. M., Dallacasa, D., & Stanghellini, C. 2001, *MNRAS*, 325, 1109
- Arlen, T., Aune, T., Beilicke, M., et al. 2013, *ApJ*, 762, 92
- Cheung, C. C., Donato, D., Gehrels, N., Sokolovsky, K. V., & Giroletti, M. 2012, *ApJ*, 756, 33
- Chiaro, G., Salvetti, D., La Mura, G., et al. 2016, *MNRAS*, 462, 3180
- Costamante, L., Aharonian, F., & Khangulyan, D. 2007, *The First GLAST Symposium*, 921, 157
- Cover, T. M., & Hart, P. E. 1967, *IEEE Trans. Information Theory*, IT-13, 21
- Cowperthwaite, P. S., Massaro, F., D’Abrusco, R., et al. 2013, *AJ*, 146, 110

- D’Abrusco, R., Massaro, F., Ajello, M., et al. 2012, *ApJ*, 748, 68
- D’Abrusco, R., Massaro, F., Paggi, A., et al. 2013, *ApJS*, 206, 12
- Gaidos, J. A., Akerlof, C. W., Biller, S., et al. 1996, *Nature*, 383, 319
- Ghirlanda, G., Ghisellini, G., Tavecchio, F., & Foschini, L. 2010, *MNRAS*, 407, 791
- Ghirlanda, G., Ghisellini, G., Tavecchio, F., Foschini, L., & Bonnoli, G. 2011, *MNRAS*, 413, 852
- Ghisellini, G., Maraschi, L., & Tavecchio, F. 2009, *MNRAS*, 396, L105
- Ghisellini, G., & Madau, P. 1996, *MNRAS*, 280, 67
- Giroletti, M., Massaro, F., D’Abrusco, R., et al. 2016, *A&A*, 588, A141
- Hartman, R. C., Bertsch, D. L., Bloom, S. D., et al. 1999, *ApJS*, 123, 79
- Hastie, T. & Tibshirani, R. 1996, *IEEE TRANSACTIONS ON PATTERN ANALYSIS AND MACHINE INTELLIGENCE*, 18, 607
- Hovatta, T., Aller, M. F., Aller, H. D., et al. 2014, *AJ*, 147, 143
- Kovalev, Y. Y. 2009, *ApJ*, 707, L56
- Landoni, M., Massaro, F., Paggi, A., et al. 2015, *AJ*, 149, 163
- Li, H.-Z., Chen, L.-E., Jiang, Y.-G., & Yi, T.-F. 2015, *Research in Astronomy and Astrophysics*, 15, 929
- Lico, R., Giroletti, M., Orienti, M., & D’Ammando, F. 2016, *A&A*, 594, A60
- Lister, M. L., Aller, M., Aller, H., et al. 2011, *ApJ*, 742, 27
- Maraschi, L., Ghisellini, G., & Celotti, A. 1992, *ApJ*, 397, L5
- Marchesini, E. J., Masetti, N., Chavushyan, V., et al. 2016, *A&A*, 596, A10
- Masetti, N., Sbarufatti, B., Parisi, P., et al. 2013, *A&A*, 559, A58
- Massaro, F., Landoni, M., D’Abrusco, R., et al. 2015, *A&A*, 575, A124
- Massaro, F., Álvarez Crespo, N., D’Abrusco, R., et al. 2016, *Ap&SS*, 361, 337
- Massaro, F., & D’Abrusco, R. 2016, *ApJ*, 827, 67

- Massaro, F., D’Abrusco, R., Ajello, M., Grindlay, J. E., & Smith, H. A. 2011, *ApJ*, 740, L48
- Massaro, F., D’Abrusco, R., Giroletti, M., et al. 2013, *ApJS*, 207, 4
- Massaro, F., Masetti, N., D’Abrusco, R., Paggi, A., & Funk, S. 2014, *AJ*, 148, 66
- Mattox, J. R., Bertsch, D. L., Chiang, J., et al. 1996, *ApJ*, 461, 396
- Mattox, J. R., Schachter, J., Molnar, L., Hartman, R. C., & Patnaik, A. R. 1997, *ApJ*, 481, 95
- Nori, M., Giroletti, M., Massaro, F., et al. 2014, *ApJS*, 212, 3
- Padovani, P., & Giommi, P. 1995, *ApJ*, 444, 567
- Paggi, A., Massaro, F., D’Abrusco, R., et al. 2013, *ApJS*, 209, 9
- Paggi, A., Milisavljevic, D., Masetti, N., et al. 2014, *AJ*, 147, 112
- Petrov, L., Mahony, E. K., Edwards, P. G., et al. 2013, *MNRAS*, 432, 1294
- Pushkarev, A. B., & Kovalev, Y. Y. 2012, *A&A*, 544, A34
- Ricci, F., Massaro, F., Landoni, M., et al. 2015, *AJ*, 149, 160
- Sambruna, R. M., Maraschi, L., & Urry, C. M. 1996, *ApJ*, 463, 444
- Schinzel, F. K., Petrov, L., Taylor, G. B., et al. 2015, *ApJS*, 217, 4
- Shaw, M. S., Filippenko, A. V., Romani, R. W., Cenko, S. B., & Li, W. 2013b, *AJ*, 146, 127
- Shaw, M. S., Romani, R. W., Cotter, G., et al. 2013a, *ApJ*, 764, 135
- Sikora, M., Stawarz, Ł., Moderski, R., Nalewajko, K., & Madejski, G. M. 2009, *ApJ*, 704, 38
- Urry, C. M., & Padovani, P. 1995, *PASP*, 107, 803
- Xie, G. Z., Ding, S. X., Dai, H., Liang, E. W., & Liu, H. T. 2003, *International Journal of Modern Physics D*, 12, 781
- Xie, G. Z., Zhou, S. B., Dai, B. Z., et al. 2002, *MNRAS*, 329, 689
- Zhang, J., Liang, E.-W., Zhang, S.-N., & Bai, J. M. 2012, *ApJ*, 752, 157
- Zhang, J., Sun, X.-N., Liang, E.-W., et al. 2014, *ApJ*, 788, 104
- Zhang, J., Xue, Z.-W., He, J.-J., Liang, E.-W., & Zhang, S.-N. 2015, *ApJ*, 807, 51

Zhao, Y., Yuan, Q., Bi, X.-J., Zhu, F.-R., & Jia, H.-Y. 2016, *International Journal of Modern Physics D*, 25, 1650006

Table 1. Data of the *Fermi*/LAT Blazar Candidates (583 Sources)

LAT Name	Counterpart Name	Class	$\log \nu_s$	$\Gamma_\gamma$	$\alpha_{r\gamma}$	$\alpha_{rx}$	$\alpha_{ox}$	$\rho_s^1$	$\rho_s^2$	$\rho_s^3$	IT
J2250.3-4206	PMN J2250-4206	BCU I	13.92	2.034	0.750	–	–	0.45	–	–	
J1647.4+4950	SBS 1646+499	BCU I	13.68	2.429	0.759	0.662	1.693	-0.20	-0.38	0.10	Q
J1412.0+5249	SBS 1410+530	BCU I	15.364	2.562	0.875	0.776	2.181	-0.90	-0.88	-0.41	
J0343.3+3622	OE 367	BCU I	12.28	2.426	0.828	–	–	-0.73	–	–	Q
J0647.6-6058	PMN J0647-6058	BCU I	13.11	2.337	0.759	–	–	-0.07	–	–	
J0040.5-2339	PMN J0040-2340	BCU I	14.358	1.946	0.768	–	–	0.40	–	–	
J2040.2-7115	PKS 2035-714	BCU I	16.15	1.798	0.795	0.624	–	0.32	0.49	–	
J0151.0-3609	PMN J0151-3605	BCU I	–	2.459	0.772	–	–	-0.35	–	–	
J2336.5+2356	B2 2334+23	BCU I	–	2.134	0.822	0.639	–	-0.24	0.09	–	
J0132.5-0802	PKS 0130-083	BCU I	15.75	1.753	0.807	0.632	1.409	0.28	0.49	-0.31	
J0618.9-1138	TXS 0616-116	BCU I	13.75	2.470	0.822	–	–	-0.75	–	–	
J1416.0+1325	PKS B1413+135	BCU I	12.865	2.363	0.843	–	–	-0.68	–	–	
J0059.1-5701	PKS 0056-572	BCU I	12.77	2.616	0.827	0.682	1.004	-0.87	-0.64	-0.70	
J0749.4+1059	TXS 0746+110	BCU I	14.265	2.203	0.795	–	–	-0.16	–	–	
J1604.4-4442	PMN J1604-4441	BCU I	12.947	2.453	0.793	–	–	-0.50	–	–	
J1131.9-0503	PKS 1128-047	BCU I	12.865	2.658	0.835	–	–	-0.94	–	–	
J1824.4+4310	1RXS J182418.7+430954	BCU I	14.929	1.725	0.747	0.519	0.627	0.74	0.85	0.35	
J0434.4-2341	PMN J0434-2342	BCU I	–	2.346	0.756	–	–	-0.06	–	–	B
J1338.6-2403	PKS 1336-237	BCU I	13.66	2.576	0.830	–	–	-0.87	–	–	
J1650.2-5044	PMN J1650-5044	BCU I	12.725	2.296	0.794	–	–	-0.31	–	–	
J1129.4-4215	SUMSS J113006-421441	BCU I	–	2.483	0.816	0.589	1.215	-0.73	-0.18	-0.49	B
J2246.7-5205	RBS 1895	BCU I	–	1.442	0.695	0.425	0.825	0.98	0.97	0.85	
J0050.0-4458	PMN J0049-4457	BCU I	13.82	2.528	0.835	0.649	1.052	-0.86	-0.44	-0.75	
J1351.7-2913	PKS 1348-289	BCU I	13.04	2.396	0.807	–	–	-0.56	–	–	
J2250.7-2806	PMN J2250-2806	BCU I	12.88	2.177	0.736	–	–	0.35	–	–	
J0040.3+4049	B3 0037+405	BCU I	–	1.132	0.773	0.566	0.715	0.68	0.77	0.07	
J1330.9+5201	87GB 132842.6+521750	BCU I	12.585	2.249	0.782	–	–	-0.14	–	–	
J1328.9-5607	PMN J1329-5608	BCU I	12.93	2.219	0.756	–	–	0.12	–	–	
J0039.0-2218	PMN J0039-2220	BCU I	16.053	1.715	0.785	0.612	1.868	0.47	0.57	-0.05	
J1315.1-5329	PMN J1315-5334	BCU I	13.775	2.281	0.802	–	–	-0.34	–	–	
J1031.0+7440	S5 1027+74	BCU I	15.6	2.147	0.795	0.649	1.386	-0.08	0.03	-0.21	
J0904.8-5734	PKS 0903-57	BCU I	14.664	2.253	0.804	–	–	-0.29	–	–	
J1512.2-2255	1RXS J151213.1-225515	BCU I	15.65	1.907	0.698	0.481	0.743	0.86	0.82	0.79	
J1007.8+0026	PKS 1005+007	BCU I	14.9	2.089	0.822	0.736	1.688	-0.17	-0.24	-0.32	
J1828.9-2417	1RXS J182853.8-241746	BCU I	16.456	1.985	0.742	0.574	–	0.58	0.49	–	
J0133.2-5159	PKS 0131-522	BCU I	12.063	2.628	0.884	0.754	0.809	-0.93	-0.85	-0.85	
J1003.6+2608	PKS 1000+26	BCU I	14.02	2.292	0.834	–	–	-0.55	–	–	B
J0134.5+2638	1RXS J013427.2+263846	BCU I	15.81	1.991	0.707	0.541	1.124	0.75	0.57	0.63	
J1543.5+0451	CGCG 050-083	BCU I	14.7	1.985	0.799	0.696	2.299	0.14	0.05	-0.10	
J0725.8-0054	PKS 0723-008	BCU I	13.355	2.189	0.823	–	–	-0.33	–	–	
J0147.0-5204	PKS 0144-522	BCU I	14.9	2.200	0.814	0.709	1.870	-0.28	-0.32	-0.22	
J0207.9-3846	PKS 0205-391	BCU I	13.495	2.544	0.826	–	–	-0.83	–	–	
J1159.3-2226	PKS 1156-221	BCU I	12.865	2.372	0.810	–	–	-0.54	–	–	
J0152.2+3707	B2 0149+37	BCU I	13.67	2.406	0.826	–	–	-0.70	–	–	
J1640.9+1142	TXS 1638+118	BCU I	14.89	2.296	0.814	–	–	-0.44	–	–	
J1239.4+0727	PKS 1236+077	BCU I	12.865	2.398	0.826	0.759	1.002	-0.69	-0.73	-0.69	



Table 1—Continued

LAT Name	Counterpart Name	Class	$\log \nu_s$	$\Gamma_\gamma$	$\alpha_{r\gamma}$	$\alpha_{rx}$	$\alpha_{ox}$	$\rho_s^1$	$\rho_s^2$	$\rho_s^3$	IT
J2235.6-2319	PMN J2236-2309	BCU I	12.38	2.817	0.839	–	–	-0.93	–	–	
J0205.0+1510	4C 15.05	BCU I	12.445	2.530	0.881	–	–	-0.88	–	–	
J1306.8-2146	PKS 1304-215	BCU I	12.41	2.147	0.812	–	–	-0.19	–	–	
J0003.8-1151	PKS 0001-121	BCU I	–	2.023	0.822	–	–	-0.08	–	–	
J0210.7-5101	PKS 0208-512	BCU I	13.12	2.170	0.805	0.814	1.272	-0.18	-0.55	-0.32	
J0827.2-0711	PMN J0827-0708	BCU I	16.085	2.067	0.779	0.584	1.047	0.16	0.36	-0.11	B
J0226.5-4442	RBS 318	BCU I	16.3	1.955	0.691	0.456	0.570	0.82	0.78	0.72	
J1302.6+5748	TXS 1300+580	BCU I	11.96	2.272	0.826	0.777	0.761	-0.47	-0.63	-0.53	
J0153.4+7114	TXS 0149+710	BCU I	15.69	1.567	0.817	0.663	–	0.34	0.50	–	
J0131.3+5548	TXS 0128+554	BCU I	–	1.904	0.784	0.642	–	0.32	0.35	–	
J1259.0-2310	PKS B1256-229	BCU I	13.452	2.029	0.803	–	–	0.05	–	–	
J1941.2-6210	PKS 1936-623	BCU I	13.12	2.432	0.832	–	–	-0.76	–	–	
J2118.0-3241	NVSS J211754-324326	BCU I	15.44	2.311	0.739	0.541	1.011	0.10	0.14	0.45	B
J1256.3-1146	PMN J1256-1146	BCU I	15.698	1.907	0.729	0.593	1.953	0.75	0.49	0.22	
J0009.6-3211	IC 1531	BCU I	14.645	2.310	0.830	0.762	2.530	-0.57	-0.65	-0.19	
J2023.2+3154	4C 31.56	BCU I	13.382	2.071	0.855	–	–	-0.32	–	–	
J2025.2+3340	B2 2023+33	BCU I	12.305	2.712	0.802	–	–	-0.75	–	–	
J0339.2-1738	PKS 0336-177	BCU I	15.48	1.928	0.768	0.608	1.787	0.42	0.43	0.05	
J0602.2+5314	GB6 J0601+5315	BCU I	15.03	2.033	0.730	0.476	1.408	0.61	0.66	0.38	
J1224.6-8312	PKS 1221-82	BCU I	11.95	2.695	0.834	–	–	-0.93	–	–	
J0522.9-3628	PKS 0521-36	BCU I	13.58	2.341	0.857	0.756	1.482	-0.68	-0.67	-0.58	Q
J2159.2-2841	NVSS J215910-284115	BCU I	14.335	1.938	0.714	–	–	0.79	–	–	
J0746.9+8511	NVSS J074715+851208	BCU II	16.28	1.787	0.693	0.530	0.886	0.93	0.79	0.84	
J0921.0-2258	NVSS J092057-225721	BCU II	15.437	1.553	0.720	0.440	0.618	0.91	0.98	0.58	B
J1630.8+1047	MG1 J163119+1051	BCU II	13.355	2.804	0.807	–	–	-0.81	–	–	
J0648.1+1606	1RXS J064814.1+160708	BCU II	16.3	1.775	0.730	0.515	–	0.85	0.85	–	
J1913.9+4441	1RXS J191401.9+443849	BCU II	15.7	1.851	0.701	0.478	0.739	0.90	0.88	0.79	B
J1935.5+8355	6C B194425+834912	BCU II	12.52	2.348	0.830	–	–	-0.63	–	–	
J0928.7+7300	GB6 J0929+7304	BCU II	13.738	2.916	0.841	–	–	-0.93	–	–	
J0928.7+7300	4C 73.07	BCU II	13.138	2.916	0.877	–	–	-0.98	–	–	
J1612.4-3100	NVSS J161219-305937	BCU II	14.8	1.880	0.753	–	–	0.60	–	–	
J0641.8-0319	TXS 0639-032	BCU II	12.76	2.454	0.834	–	–	-0.79	–	–	
J0256.3+0335	PKS B0253+033	BCU II	15.62	1.896	0.801	–	–	0.20	–	–	
J1607.9-2040	NVSS J160756-203942	BCU II	14.055	2.015	0.792	–	–	0.14	–	–	
J0939.2-1732	TXS 0936-173	BCU II	13.004	2.270	0.792	–	–	-0.26	–	–	
J1636.7+2624	NVSS J163651+262657	BCU II	14.685	2.039	0.724	–	–	0.62	–	–	B
J0732.2-4638	PKS 0731-465	BCU II	13.32	2.354	0.840	0.740	0.537	-0.66	-0.64	-0.42	
J0756.3-6433	SUMSS J075625-643031	BCU II	15.867	2.217	0.705	–	–	0.43	–	–	
J0917.3-0344	NVSS J091714-034315	BCU II	15.6	1.764	0.734	0.536	0.977	0.83	0.79	0.51	
J1944.1-4523	1RXS J194422.6-452326	BCU II	16.14	1.560	0.764	0.545	1.130	0.68	0.82	0.08	
J0728.0+4828	GB6 J0727+4827	BCU II	14.54	2.371	0.794	–	–	-0.41	–	–	B
J1559.7+8512	WN B1609.6+8517	BCU II	14.6	2.351	0.775	0.733	1.069	-0.24	-0.62	-0.06	
J1557.4-7040	PKS 1552-705	BCU II	14.12	2.301	0.797	–	–	-0.33	–	–	
J0947.1-2542	1RXS J094709.2-254056	BCU II	15.84	1.950	0.721	0.543	0.939	0.76	0.62	0.64	
J0734.3-7709	PKS 0736-770	BCU II	12.515	2.290	0.762	–	–	-0.03	–	–	
J1550.3+7409	87GB 155014.9+741816	BCU II	14.413	2.688	0.791	–	–	-0.67	–	–	

Table 1—Continued

LAT Name	Counterpart Name	Class	$\log \nu_s$	$\Gamma_\gamma$	$\alpha_{r\gamma}$	$\alpha_{rx}$	$\alpha_{ox}$	$\rho_s^1$	$\rho_s^2$	$\rho_s^3$	IT
J0928.9-3530	NVSS J092849-352947	BCU II	13.775	2.530	0.725	–	–	-0.07	–	–	
J0603.8+2155	4C 22.12	BCU II	13.25	2.101	0.849	–	–	-0.33	–	–	
J1547.1-2801	1RXS J154711.8-280222	BCU II	15.556	1.708	0.742	0.572	0.799	0.79	0.71	0.45	
J0958.4-6752	1RXS J095812.8-675241	BCU II	15.95	2.207	0.742	0.469	0.819	0.26	0.43	0.47	
J0730.5-0537	TXS 0728-054	BCU II	15.2	2.100	0.775	–	–	0.15	–	–	
J0712.2-6436	MRC 0712-643	BCU II	13.244	2.383	0.865	0.835	0.889	-0.75	-0.80	-0.87	
J0746.6-4756	PMN J0746-4755	BCU II	15.3	2.254	0.744	–	–	0.16	–	–	B
J0744.8-4028	PMN J0744-4032	BCU II	12.62	2.340	0.746	–	–	0.00	–	–	
J1626.4-7640	PKS 1619-765	BCU II	14.08	1.990	0.766	–	–	0.37	–	–	B
J1628.2+7703	6C B163030.4+771303	BCU II	13.56	2.449	0.821	–	–	-0.73	–	–	
J0748.8+4929	NVSS J074837+493040	BCU II	13.811	2.339	0.752	–	–	-0.03	–	–	
J1007.4-3334	TXS 1005-333	BCU II	13.74	2.538	0.846	–	–	-0.90	–	–	
J0748.0-1639	TXS 0745-165	BCU II	11.92	2.605	0.832	–	–	-0.90	–	–	
J0703.4-3914	1RXS J070312.7-391417	BCU II	14.05	2.288	0.733	0.638	1.289	0.17	-0.13	0.42	
J1009.0-3137	PKS 1006-313	BCU II	14.16	2.348	0.797	–	–	-0.41	–	–	
J1532.7-1319	TXS 1530-131	BCU II	12.725	2.094	0.726	–	–	0.55	–	–	
J0700.3-6310	SUMSS J065958-631238	BCU II	14.23	1.994	0.758	–	–	0.44	–	–	
J0658.3-5832	PMN J0658-5840	BCU II	13.74	2.402	0.838	–	–	-0.73	–	–	
J0658.3-5832	PMN J0658-5824	BCU II	13.74	2.402	0.835	–	–	-0.72	–	–	
J1014.2+4115	GB6 J1014+4112	BCU II	13.67	2.424	0.770	–	–	-0.29	–	–	
J1016.0-0635	NVSS J101626-063624	BCU II	13.425	2.544	0.770	–	–	-0.41	–	–	
J1536.6+8331	NVSS J153556+832614	BCU II	13.145	2.481	0.806	–	–	-0.65	–	–	
J1518.0-2732	TXS 1515-273	BCU II	15.15	2.133	0.778	–	–	0.08	–	–	
J0912.6-2757	PMN J0912-2752	BCU II	15.056	2.697	0.821	–	–	-0.86	–	–	
J0651.3+4014	RX J0651.0+4013	BCU II	15.45	2.120	0.736	0.527	0.923	0.44	0.43	0.47	
J0803.3-0339	TXS 0800-034	BCU II	15.7	1.996	0.764	–	–	0.38	–	–	
J0649.6-3138	1RXS J064933.8-313914	BCU II	18	1.729	0.667	0.377	0.484	0.93	0.95	0.78	
J1514.8-3623	PMN J1514-3617	BCU II	12.59	2.405	0.826	–	–	-0.69	–	–	
J1512.3+8005	1RXS J151026.3+795946	BCU II	13.425	2.513	0.811	0.724	0.887	-0.70	-0.72	-0.47	
J0852.6-5756	PMN J0852-5755	BCU II	13.076	2.403	0.788	0.702	–	-0.40	-0.52	–	
J0723.7+2050	GB6 J0723+2051	BCU II	15.85	2.400	0.759	–	–	-0.17	–	–	
J0646.4-5452	PMN J0646-5451	BCU II	13.635	2.189	0.811	–	–	-0.25	–	–	
J1509.9-2951	TXS 1507-296	BCU II	14.65	2.782	0.839	–	–	-0.94	–	–	
J1024.8+0105	PMN J1024+0056	BCU II	13.6	2.549	0.795	–	–	-0.60	–	–	
J1704.0+7646	NVSS J170357+764611	BCU II	13.148	2.574	0.782	–	–	-0.52	–	–	
J1507.6-3710	NVSS J150720-370903	BCU II	14.48	2.131	0.761	–	–	0.22	–	–	
J1028.0+1829	GB6 J1027+1831	BCU II	11.99	2.236	0.760	–	–	0.06	–	–	
J0730.5-6606	PMN J0730-6602	BCU II	15.25	1.789	0.745	0.548	1.183	0.73	0.75	0.32	B
J0940.7-6102	MRC 0939-608	BCU II	13.671	2.421	0.816	–	–	-0.66	–	–	
J0939.9-2831	TXS 0937-282	BCU II	12.54	2.471	0.810	–	–	-0.67	–	–	
J1035.2+5545	GB6 J1035+5542	BCU II	13.53	2.943	0.830	–	–	-0.90	–	–	
J2024.4-0848	1RXS J202428.9-084810	BCU II	14.76	1.703	0.717	0.514	0.787	0.92	0.88	0.71	
J1714.1-2029	1RXS J171405.2-202747	BCU II	16.35	1.344	0.680	0.359	0.946	0.99	1.00	0.86	
J1040.4+0615	GB6 J1040+0617	BCU II	13.775	2.226	0.704	–	–	0.43	–	–	B
J2031.0+1937	RX J2030.8+1935	BCU II	15.59	1.826	0.731	–	–	0.83	–	–	B
J1040.8+1342	1RXS J104057.7+134216	BCU II	16.15	1.760	0.689	0.480	0.679	0.94	0.92	0.81	B

Table 1—Continued

LAT Name	Counterpart Name	Class	$\log \nu_s$	$\Gamma_\gamma$	$\alpha_{r\gamma}$	$\alpha_{rx}$	$\alpha_{ox}$	$\rho_s^1$	$\rho_s^2$	$\rho_s^3$	IT
J1040.9-1205	NVSS J104108-120332	BCU II	15.35	2.107	0.718	–	–	0.56	–	–	
J2033.6+6309	87GB 203249.5+625814	BCU II	13.25	1.895	0.772	–	–	0.42	–	–	
J1042.0-0557	PMN J1042-0558	BCU II	15	1.944	0.768	–	–	0.41	–	–	
J0333.4+7853	NVSS J033344+785027	BCU II	14.82	2.198	0.764	–	–	0.10	–	–	
J0618.2-2429	PMN J0618-2426	BCU II	15	2.417	0.836	–	–	-0.75	–	–	Q
J1042.1-4126	1RXS J104204.1-412936	BCU II	15.35	1.976	0.731	–	–	0.65	–	–	
J1446.8-1831	NVSS J144644-182922	BCU II	15.95	1.723	0.728	0.582	–	0.88	0.68	–	
J2040.0-5734	PKS 2036-577	BCU II	12.48	2.269	0.849	–	–	-0.58	–	–	
J1716.7-8112	1RXS J171712.6-811501	BCU II	15.75	2.060	0.785	0.578	1.339	0.14	0.38	-0.10	
J0923.1+3853	B2 0920+39	BCU II	12.585	2.752	0.838	–	–	-0.94	–	–	
J0611.2+4323	NVSS J061107+432404	BCU II	15.6	2.168	0.740	0.583	–	0.34	0.22	–	
J1719.3+1206	1RXS J171921.2+120711	BCU II	14.68	2.078	0.747	0.630	0.849	0.41	0.17	0.38	
J1427.8-3215	NVSS J142750-321515	BCU II	14.384	2.036	0.711	–	–	0.70	–	–	
J2046.7-1011	PMN J2046-1010	BCU II	15.02	1.609	0.770	0.684	1.177	0.62	0.42	0.04	
J2049.0-6801	PKS 2043-682	BCU II	14.975	2.059	0.808	–	–	-0.02	–	–	
J1723.5-5609	PMN J1723-5614	BCU II	15.007	2.618	0.807	–	–	-0.74	–	–	
J1421.0-1122	PMN J1420-1118	BCU II	13.285	2.064	0.744	–	–	0.46	–	–	
J0604.7-4849	1RXS J060432.7-485007	BCU II	14.3	2.399	0.818	0.748	0.873	-0.65	-0.71	-0.54	
J0855.2-0718	PKS 0852-07	BCU II	14.156	2.565	0.869	–	–	-0.90	–	–	
J1418.9+7731	1RXS J141901.8+773229	BCU II	15.9	1.906	0.682	0.478	0.892	0.86	0.82	0.88	
J2051.8-5535	PMN J2052-5533	BCU II	12.77	2.577	0.828	–	–	-0.86	–	–	
J1418.5+3543	NVSS J141828+354250	BCU II	14.075	2.058	0.698	–	–	0.71	–	–	
J1330.1-7002	PKS 1326-697	BCU II	13.425	2.223	0.744	–	–	0.22	–	–	
J2103.9-3546	NVSS J210353-354620	BCU II	13.46	2.363	0.754	–	–	-0.07	–	–	
J1407.7-4256	SUMSS J140739-430231	BCU II	12.917	2.137	0.789	–	–	-0.02	–	–	
J1406.0-2508	NVSS J140609-250808	BCU II	15.1	1.893	0.715	–	–	0.84	–	–	B
J0055.2-1213	TXS 0052-125	BCU II	12.305	2.397	0.825	–	–	-0.69	–	–	
J2106.1+2505	MG3 J210642+2501	BCU II	13.32	2.528	0.797	–	–	-0.60	–	–	
J1356.3-4029	SUMSS J135625-402820	BCU II	14.055	2.060	0.761	–	–	0.32	–	–	
J1125.0-2101	PMN J1125-2100	BCU II	15.55	1.784	0.725	0.598	1.199	0.88	0.57	0.48	B
J1503.7-6426	AT20G J150350-642539	BCU II	13.285	2.331	0.752	–	–	-0.01	–	–	
J1126.7-3834	PKS 1124-382	BCU II	12.515	2.260	0.824	–	–	-0.45	–	–	
J1346.9-2958	NVSS J134706-295840	BCU II	14.72	1.744	0.709	–	–	0.93	–	–	B
J1723.7-7713	PKS 1716-771	BCU II	13.355	2.471	0.803	–	–	-0.61	–	–	
J1344.5-3655	PKS 1341-366	BCU II	14.44	2.182	0.824	–	–	-0.33	–	–	
J0535.6-2749	PMN J0535-2751	BCU II	13.22	2.415	0.813	–	–	-0.63	–	–	
J1637.6-3449	NVSS J163750-344915	BCU II	13	1.732	0.739	0.599	–	0.81	0.61	–	
J1735.4-1118	PMN J1735-1117	BCU II	13.845	2.156	0.742	–	–	0.35	–	–	
J1838.5-6006	SUMSS J183806-600033	BCU II	15.41	1.857	0.756	–	–	0.59	–	–	
J0045.2-3704	PKS 0042-373	BCU II	12.76	2.543	0.810	–	–	-0.72	–	–	
J0356.3-6948	PMN J0357-6948	BCU II	13	2.530	0.809	–	–	-0.70	–	–	
J0529.8-7242	PKS 0530-727	BCU II	13.18	2.475	0.807	0.765	1.258	-0.65	-0.79	-0.36	
J1138.2+4905	GB6 J1138+4858	BCU II	12.935	2.850	0.794	–	–	-0.73	–	–	
J1331.1-1328	PMN J1331-1326	BCU II	14.055	2.374	0.752	–	–	-0.08	–	–	
J0526.6+6321	GB6 J0526+6317	BCU II	13.6	2.540	0.783	–	–	-0.51	–	–	
J1141.2+6805	1RXS J114118.3+680433	BCU II	15.65	1.611	0.727	0.656	1.024	0.89	0.50	0.56	

Table 1—Continued

LAT Name	Counterpart Name	Class	$\log \nu_s$	$\Gamma_\gamma$	$\alpha_{r\gamma}$	$\alpha_{rx}$	$\alpha_{ox}$	$\rho_s^1$	$\rho_s^2$	$\rho_s^3$	IT
J1141.6-1406	1RXS J114142.2-140757	BCU II	16.19	2.176	0.753	0.584	0.870	0.23	0.20	0.31	B
J1736.0+2033	NVSS J173605+203301	BCU II	15.05	1.722	0.697	–	–	0.96	–	–	B
J1021.8+8023	NVSS J102201+802350	BCU II	13.215	2.327	0.796	–	–	-0.37	–	–	
J1740.4+5347	NVSS J174036+534623	BCU II	13.915	2.019	0.754	–	–	0.43	–	–	
J0526.0+4253	NVSS J052520+425520	BCU II	13.145	2.436	0.737	–	–	-0.04	–	–	
J0521.7+0103	NVSS J052140+010257	BCU II	13.56	1.699	0.719	–	–	0.92	–	–	
J1753.5-5010	PMN J1753-5015	BCU II	13.617	2.505	0.796	–	–	-0.58	–	–	
J1319.6+7759	NVSS J131921+775823	BCU II	14.435	1.785	0.722	–	–	0.89	–	–	
J1318.7-1232	PMN J1318-1235	BCU II	13.45	2.348	0.744	–	–	0.00	–	–	
J0836.3+2143	MG2 J083615+2138	BCU II	12.585	2.566	0.809	–	–	-0.72	–	–	
J1154.0-3243	PKS 1151-324	BCU II	13.2	2.053	0.759	–	–	0.35	–	–	
J1825.2-5230	PKS 1821-525	BCU II	13.32	2.017	0.766	–	–	0.34	–	–	
J1155.4-3417	NVSS J115520-341718	BCU II	15.8	1.335	0.731	–	–	0.86	–	–	
J0241.3+6542	TXS 0237+655	BCU II	15.5	2.080	0.756	0.613	–	0.32	0.23	–	
J1757.1+1533	87GB 175437.6+153548	BCU II	12.83	2.045	0.787	–	–	0.13	–	–	
J1759.1-4822	PMN J1758-4820	BCU II	13.25	2.296	0.764	–	–	-0.06	–	–	
J1539.8-1128	PMN J1539-1128	BCU II	16.35	2.085	0.757	0.536	0.871	0.32	0.46	0.25	
J2141.6-6412	PMN J2141-6411	BCU II	13.852	2.495	0.775	–	–	-0.41	–	–	
J0028.6+7507	GB6 J0028+7506	BCU II	14.23	2.341	0.763	–	–	-0.11	–	–	
J1844.3+1547	NVSS J184425+154646	BCU II	14.708	2.028	0.720	–	–	0.67	–	–	B
J1820.3+3625	NVSS J182021+362343	BCU II	16.085	1.777	0.710	0.539	0.883	0.92	0.77	0.76	
J1200.8+1228	GB6 J1200+1230	BCU II	13.53	2.248	0.750	–	–	0.11	–	–	B
J1200.9+2010	TXS 1158+204	BCU II	12.69	2.524	0.799	–	–	-0.62	–	–	
J1819.1+4259	NVSS J181927+425800	BCU II	13.81	2.512	0.744	–	–	-0.18	–	–	
J1203.5-3925	PMN J1203-3926	BCU II	15.85	1.639	0.748	0.573	0.884	0.77	0.74	0.35	
J1307.6-4300	1RXS J130737.8-425940	BCU II	15.497	1.837	0.681	0.499	1.050	0.89	0.84	0.80	
J0506.9-5435	1ES 0505-546	BCU II	16.14	1.603	0.685	0.414	0.756	0.98	0.98	0.85	
J0021.6-6835	PKS 0021-686	BCU II	13.44	2.652	0.883	0.746	1.144	-0.94	-0.85	-0.93	
J1819.1+2134	MG2 J181902+2132	BCU II	14.985	2.251	0.763	–	–	0.01	–	–	B
J1816.9-4944	PMN J1816-4943	BCU II	13.04	1.944	0.796	–	–	0.19	–	–	
J1304.9-2109	PKS B1302-208	BCU II	14.055	2.148	0.830	–	–	-0.30	–	–	
J1304.2-2411	PMN J1304-2412	BCU II	14.49	1.957	0.734	–	–	0.66	–	–	
J2156.0+1818	RX J2156.0+1818	BCU II	14.864	1.914	0.725	0.507	0.847	0.78	0.75	0.66	B
J1942.7+1033	1RXS J194246.3+103339	BCU II	15.435	1.818	0.703	0.537	–	0.91	0.76	–	B
J1300.2+1416	NVSS J130041+141728	BCU II	13.05	2.855	0.789	–	–	-0.70	–	–	
J0426.6+0459	4C 4.15	BCU II	14.2	2.555	0.849	–	–	-0.91	–	–	
J1259.8-3749	NVSS J125949-374856	BCU II	14.626	2.242	0.722	–	–	0.32	–	–	B
J2000.1+4212	MG4 J195957+4213	BCU II	12.55	2.468	0.801	–	–	-0.60	–	–	
J0456.3+2702	MG2 J045613+2702	BCU II	13.285	2.460	0.762	–	–	-0.27	–	–	
J2200.9-2412	NVSS J220036-241428	BCU II	13.852	2.454	0.755	–	–	-0.20	–	–	
J0829.6-1137	NVSS J082939-114103	BCU II	14.16	1.890	0.749	–	–	0.63	–	–	
J1807.8+6427	7C 1807+6428	BCU II	14.437	2.092	0.770	–	–	0.20	–	–	
J2018.5+3851	TXS 2016+386	BCU II	13.508	2.229	0.757	–	–	0.08	–	–	
J2056.7+4938	RGB J2056+496	BCU II	15.742	1.783	0.737	0.513	–	0.80	0.85	–	
J2212.3-7039	PMN J2211-7039	BCU II	15.03	2.759	0.781	–	–	-0.61	–	–	
J2212.6+2801	MG3 J221240+2759	BCU II	13.88	1.790	0.767	–	–	0.56	–	–	

Table 1—Continued

LAT Name	Counterpart Name	Class	$\log \nu_s$	$\Gamma_\gamma$	$\alpha_{r\gamma}$	$\alpha_{rx}$	$\alpha_{ox}$	$\rho_s^1$	$\rho_s^2$	$\rho_s^3$	IT
J1251.0-0203	TXS 1248-017	BCU II	13.272	2.386	0.784	–	–	-0.34	–	–	
J1225.7-7314	PMN J1225-7313	BCU II	14.825	2.309	0.803	–	–	-0.40	–	–	
J2220.3+2812	RX J2220.4+2814	BCU II	15.55	1.833	0.752	0.574	1.302	0.64	0.63	0.23	
J1244.3-4955	SUMSS J124422-495422	BCU II	14.726	2.188	0.773	–	–	0.03	–	–	
J1243.9-0217	PMN J1243-0218	BCU II	12.83	2.186	0.771	–	–	0.05	–	–	
J0440.3+1444	TXS 0437+145	BCU II	13.04	2.395	0.785	–	–	-0.37	–	–	
J0439.9-1859	PMN J0439-1900	BCU II	15.056	1.919	0.740	–	–	0.68	–	–	B
J0439.6-3159	1RXS J043931.4-320045	BCU II	15.315	1.771	0.701	0.490	0.708	0.95	0.91	0.76	
J1238.2-1958	PMN J1238-1959	BCU II	14.075	2.349	0.769	0.654	1.159	-0.18	-0.26	0.03	B
J2230.5-7817	PKS 2225-785	BCU II	14.985	2.508	0.823	–	–	-0.78	–	–	
J2347.9+5436	NVSS J234753+543627	BCU II	16.4	1.733	0.717	0.443	–	0.92	0.96	–	
J1136.1-7411	PKS 1133-739	BCU II	13.04	2.484	0.839	–	–	-0.84	–	–	
J0434.6+0921	TXS 0431+092	BCU II	14.655	2.115	0.766	–	–	0.21	–	–	
J2232.9-2021	1RXS J223249.5-202232	BCU II	16.58	2.081	0.710	0.492	0.931	0.64	0.56	0.75	B
J0433.7-6028	PKS 0432-606	BCU II	13.46	2.509	0.806	0.801	1.720	-0.65	-0.88	-0.21	Q
J2233.5-1235	PKS 2231-127	BCU II	14.755	2.373	0.838	–	–	-0.68	–	–	
J0433.1+3228	NVSS J043307+322840	BCU II	16.085	1.968	0.703	0.494	0.803	0.79	0.72	0.83	B
J0431.6+7403	GB6 J0431+7403	BCU II	15.62	1.988	0.717	0.573	0.895	0.74	0.49	0.70	
J0430.5+1655	MG1 J043022+1655	BCU II	14.72	2.402	0.733	–	–	0.02	–	–	
J2234.1-2655	PMN J2234-2656	BCU II	13.513	2.187	0.773	0.721	1.052	0.03	-0.35	-0.02	
J0429.8+2843	MG2 J042948+2843	BCU II	14.28	1.963	0.742	–	–	0.61	–	–	
J1238.3-4543	PMN J1238-4541	BCU II	14.2	2.153	0.765	–	–	0.15	–	–	
J0427.3-3900	PMN J0427-3900	BCU II	13.72	2.672	0.770	–	–	-0.50	–	–	
J0002.2-4152	1RXS J000135.5-415519	BCU II	15.8	2.089	0.720	–	–	0.58	–	–	
J0426.3+6827	4C 68.05	BCU II	13.4	2.378	0.815	–	–	-0.60	–	–	
J0505.5-1558	TXS 0503-160	BCU II	13.985	2.102	0.821	0.769	1.074	-0.18	-0.37	-0.62	
J2236.2-5049	SUMSS J223605-505521	BCU II	13.2	2.607	0.769	–	–	-0.45	–	–	
J2149.6+1915	TXS 2147+191	BCU II	13.145	2.569	0.782	–	–	-0.52	–	–	
J0508.2-1936	PMN J0508-1936	BCU II	13.075	2.375	0.780	–	–	-0.31	–	–	Q
J2144.2+3132	MG3 J214415+3132	BCU II	14.96	2.362	0.762	–	–	-0.14	–	–	
J2142.2-2546	PMN J2142-2551	BCU II	13.569	2.231	0.796	–	–	-0.21	–	–	
J2243.2-3933	NVSS J224326-393353	BCU II	13.215	2.119	0.763	–	–	0.23	–	–	
J0515.3-4557	PMN J0514-4554	BCU II	13.18	2.437	0.825	–	–	-0.73	–	–	
J2133.8+6648	NVSS J213349+664706	BCU II	15.8	2.078	0.702	–	–	0.68	–	–	
J2133.3+2533	87GB 213100.1+251534	BCU II	14.64	2.010	0.743	–	–	0.53	–	–	
J2132.4-5420	PMN J2132-5420	BCU II	12.69	2.634	0.764	–	–	-0.42	–	–	
J0519.5+0852	TXS 0516+087	BCU II	12.62	2.785	0.780	–	–	-0.62	–	–	
J2246.2+1547	NVSS J224604+154437	BCU II	14.95	2.183	0.751	–	–	0.23	–	–	
J0003.2-5246	RBS 6	BCU II	16.85	1.895	0.763	0.548	0.661	0.50	0.65	0.20	
J0003.8-1151	PMN J0004-1148	BCU II	12.515	2.023	0.830	–	–	-0.13	–	–	B
J2126.5-3926	PMN J2126-3921	BCU II	14.265	2.203	0.778	–	–	-0.04	–	–	
J1038.9-5311	MRC 1036-529	BCU II	12.235	2.320	0.816	–	–	-0.50	–	–	Q
J2110.3+3540	B2 2107+35A	BCU II	14.048	2.645	0.862	0.629	–	-0.95	-0.46	–	
J2251.5-4928	SUMSS J225128-492912	BCU II	14.23	1.967	0.719	–	–	0.75	–	–	
J0529.1+0933	GB6 J0529+0934	BCU II	16.456	2.317	0.722	0.430	0.414	0.21	0.36	0.46	
J2119.2-3313	PMN J2118-3316	BCU II	12.69	2.352	0.764	–	–	-0.14	–	–	

Table 1—Continued

LAT Name	Counterpart Name	Class	$\log \nu_s$	$\Gamma_\gamma$	$\alpha_{r\gamma}$	$\alpha_{rx}$	$\alpha_{ox}$	$\rho_s^1$	$\rho_s^2$	$\rho_s^3$	IT
J0357.1+2325	MG3 J035721+2319	BCU II	12.95	2.411	0.799	–	–	-0.51	–	–	
J2108.0+3654	TXS 2106+367	BCU II	14.86	1.934	0.751	–	–	0.57	–	–	B
J0532.0-4827	PMN J0531-4827	BCU II	13.11	2.031	0.690	0.757	–	0.75	-0.24	–	
J0533.0-3939	PKS 0531-397	BCU II	13.145	2.488	0.799	–	–	-0.60	–	–	
J2114.7+3130	B2 2112+31	BCU II	12.62	2.349	0.821	–	–	-0.59	–	–	
J2258.1-8248	PMN J2258-8246	BCU II	15.12	2.194	0.740	–	–	0.30	–	–	
J2112.7+0819	1RXS J211242.5+081831	BCU II	15.728	1.806	0.699	0.469	–	0.92	0.91	–	
J0538.4-3909	NVSS J053810-390844	BCU II	14.42	2.041	0.731	0.558	0.943	0.59	0.47	0.54	
J2109.1-6638	PKS 2104-668	BCU II	13.967	2.006	0.785	0.659	0.935	0.21	0.17	-0.19	B
J2305.3-4219	SUMSS J230512-421859	BCU II	13.92	2.048	0.763	–	–	0.32	–	–	
J2104.2-0211	NVSS J210421-021239	BCU II	15.55	1.524	0.716	0.526	0.905	0.92	0.85	0.69	B
J0553.5-2036	NVSS J055333-203417	BCU II	15	1.985	0.777	0.673	0.998	0.28	0.14	-0.08	
J0841.3-3554	NVSS J084121-355506	BCU II	15.956	1.764	0.705	–	–	0.94	–	–	
J2103.9-6233	PMN J2103-6232	BCU II	14.864	1.975	0.723	0.543	0.887	0.72	0.58	0.65	
J0342.6-3006	PKS 0340-302	BCU II	12.68	1.846	0.798	–	–	0.26	–	–	
J2309.6-3633	1RXS J230940.6-363241	BCU II	15.81	1.854	0.755	0.603	–	0.60	0.51	–	
J1223.3-3028	NVSS J122337-303246	BCU II	15.95	1.887	0.697	–	–	0.87	–	–	
J0602.8-4016	SUMSS J060251-401845	BCU II	15	1.923	0.725	0.643	1.253	0.77	0.32	0.49	
J1254.1-2203	NVSS J125422-220413	BCU II	14.34	2.296	0.728	–	–	0.20	–	–	
J0338.5+1303	RX J0338.4+1302	BCU II	15.645	1.695	0.678	–	–	0.96	–	–	
J0606.4-4729	ESO 254-G017	BCU II	15.05	2.327	0.813	0.609	2.084	-0.49	-0.07	-0.19	
J2049.7+1002	PKS 2047+098	BCU II	12.06	2.403	0.789	–	–	-0.41	–	–	
J2316.8-5209	SUMSS J231701-521003	BCU II	14.52	1.735	0.734	–	–	0.84	–	–	
J2317.3-4534	1RXS J231733.0-453348	BCU II	15.7	2.186	0.724	0.586	0.901	0.40	0.19	0.62	B
J2318.6+1912	TXS 2315+189	BCU II	13.92	2.741	0.824	–	–	-0.88	–	–	
J0030.7-0209	PKS B0027-024	BCU II	12.576	2.378	0.789	–	–	-0.38	–	–	
J2321.2-6439	PMN J2321-6438	BCU II	14.72	2.401	0.806	–	–	-0.56	–	–	
J2036.6-3325	1RXS J203650.9-332817	BCU II	16.364	1.305	0.676	0.408	–	0.99	0.97	–	B
J2322.9-4917	SUMSS J232254-491629	BCU II	15.65	1.957	0.717	–	–	0.77	–	–	
J0729.5-3127	NVSS J072922-313128	BCU II	13.133	2.654	0.759	–	–	-0.39	–	–	
J0333.4+4003	B3 0330+399	BCU II	14.3	2.238	0.762	–	–	0.04	–	–	
J0331.3-6155	PMN J0331-6155	BCU II	15.5	2.076	0.795	0.674	1.085	0.03	0.02	-0.32	
J2026.3+7644	1RXS J202633.4+764432	BCU II	16.262	1.839	0.692	0.447	0.618	0.90	0.90	0.75	
J0326.0-1842	PMN J0325-1843	BCU II	14.405	2.205	0.792	–	–	-0.15	–	–	
J0630.3+6906	GB6 J0629+6900	BCU II	15	2.393	0.772	–	–	-0.27	–	–	
J2017.6-4110	1RXS J201731.2-411452	BCU II	16.05	2.160	0.792	–	–	-0.08	–	–	
J0643.4-5358	PMN J0643-5358	BCU II	12.97	2.444	0.765	–	–	-0.27	–	–	
J0644.3-6713	PKS 0644-671	BCU II	13.7	2.095	0.725	–	–	0.55	–	–	
J0644.6-2853	1RXS J064444.2-285120	BCU II	16.2	2.111	0.759	0.524	0.707	0.27	0.45	0.24	
J2328.4-4034	PKS 2325-408	BCU II	13.25	2.309	0.761	–	–	-0.05	–	–	Q
J0647.0-5134	1ES 0646-515	BCU II	16.45	2.189	0.768	0.456	0.689	0.08	0.48	0.15	
J0647.1-4415	SUMSS J064648-441929	BCU II	14.055	2.345	0.771	–	–	-0.20	–	–	
J1159.6-0723	PMN J1159-0723	BCU II	13.95	2.104	0.753	–	–	0.32	–	–	
J0318.7+2134	MG3 J031849+2135	BCU II	14.58	1.837	0.723	–	–	0.86	–	–	
J0654.5+0926	RX J0654.3+0925	BCU II	15.35	2.666	0.766	0.526	–	-0.45	-0.19	–	
J2014.9+1623	4C 16.67	BCU II	13.808	2.410	0.825	0.740	0.961	-0.70	-0.69	-0.65	

Table 1—Continued

LAT Name	Counterpart Name	Class	$\log \nu_s$	$\Gamma_\gamma$	$\alpha_{r\gamma}$	$\alpha_{rx}$	$\alpha_{ox}$	$\rho_s^1$	$\rho_s^2$	$\rho_s^3$	IT
J2338.7-7401	1RXS J233919.8-740439	BCU II	16.195	1.888	0.733	0.564	1.152	0.76	0.61	0.44	
J0652.0-4808	1RXS J065201.0-480858	BCU II	16.2	2.044	0.767	0.587	0.811	0.31	0.38	0.14	
J0653.6+2817	GB6 J0653+2816	BCU II	14.195	2.250	0.729	–	–	0.26	–	–	
J2014.5+0648	NVSS J201431+064849	BCU II	15.488	1.915	0.691	0.544	1.125	0.85	0.66	0.71	
J2344.4+0549	1RXS J234354.4+054713	BCU II	14.759	2.193	0.726	–	–	0.38	–	–	
J2346.7+0705	TXS 2344+068	BCU II	14.755	1.779	0.765	0.721	1.371	0.58	0.19	0.07	B
J2348.4-5100	SUMSS J234852-510311	BCU II	13.985	2.306	0.757	–	–	-0.01	–	–	
J0310.4-5015	1RXS J031036.0-501615	BCU II	16.25	1.754	0.699	0.593	1.104	0.96	0.61	0.68	
J0706.1-4849	PMN J0705-4847	BCU II	12.795	2.412	0.785	–	–	-0.40	–	–	
J2007.7-7728	PKS 2000-776	BCU II	13.04	2.683	0.808	–	–	-0.78	–	–	
J0708.9+2239	GB6 J0708+2241	BCU II	15.15	2.076	0.736	0.571	1.014	0.51	0.38	0.47	B
J2002.7+6303	1RXS J200245.4+630226	BCU II	13.655	2.127	0.714	0.479	–	0.55	0.52	–	
J0305.2-1607	PKS 0302-16	BCU II	15.57	1.688	0.840	–	–	0.15	–	–	
J1959.8-4725	SUMSS J195945-472519	BCU II	15.355	1.524	0.665	0.560	1.186	0.99	0.79	0.76	B
J0720.0-4010	1RXS J071939.2-401153	BCU II	15.8	2.228	0.755	0.541	0.888	0.11	0.25	0.25	B
J1955.0-1605	1RXS J195500.6-160328	BCU II	15.943	2.047	0.705	0.506	0.893	0.71	0.58	0.79	B
J0303.0+3150	B2 0259+31	BCU II	13.88	2.315	0.828	–	–	-0.56	–	–	
J1954.9-5640	1RXS J195503.1-564031	BCU II	15.755	1.878	0.682	0.452	0.936	0.87	0.87	0.86	
J0301.8-7157	PKS 0301-721	BCU II	13.67	2.766	0.857	–	–	-0.97	–	–	Q
J0301.8-2721	NVSS J030158-272754	BCU II	13.985	2.158	0.772	–	–	0.09	–	–	
J0301.4-1652	PMN J0301-1652	BCU II	13.72	2.151	0.795	–	–	-0.09	–	–	
J2358.3-2853	PMN J2358-2853	BCU II	13.495	2.414	0.807	–	–	-0.58	–	–	
J1256.7+5328	TXS 1254+538	BCU II	13.25	2.639	0.809	–	–	-0.77	–	–	
J1941.8+7218	87GB 194202.1+721428	BCU II	12.94	2.544	0.796	–	–	-0.61	–	–	
J1218.8-4827	PMN J1219-4826	BCU II	14.113	2.336	0.751	–	–	-0.02	–	–	
J0255.8+0532	PMN J0255+0533	BCU II	13.705	2.070	0.775	–	–	0.18	–	–	B
J0253.5+3216	MG3 J025334+3217	BCU II	12.8	2.052	0.748	–	–	0.43	–	–	Q
J0012.4+7040	TXS 0008+704	BCU II	13.075	2.484	0.836	–	–	-0.83	–	–	
J0014.6+6119	4C 60.01	BCU II	13.113	1.887	0.859	–	–	-0.13	–	–	
J0748.5+7910	JVAS J0750+7909	BCU II	12.9	2.344	0.815	–	–	-0.53	–	–	
J0015.7+5552	GB6 J0015+5551	BCU II	15.791	2.115	0.763	0.501	–	0.24	0.50	–	B
J0216.1-7016	PMN J0215-7014	BCU II	12.76	2.565	0.778	–	–	-0.49	–	–	
J1918.0+3750	1RXS J191810.2+375315	BCU II	16.35	2.192	0.711	0.459	0.755	0.45	0.47	0.72	
J0249.1+8438	NVSS J024948+843556	BCU II	13.74	2.147	0.784	–	–	0.01	–	–	
J0047.9+5447	1RXS J004754.5+544758	BCU II	15.896	1.333	0.715	0.490	–	0.91	0.90	–	
J1913.5-3631	PMN J1913-3630	BCU II	13.5	2.162	0.762	–	–	0.17	–	–	
J1912.6-1223	TXS 1909-124	BCU II	13	2.492	0.759	–	–	-0.27	–	–	
J1911.4-1908	PMN J1911-1908	BCU II	15.95	1.770	0.784	–	–	0.43	–	–	
J1904.5+3627	MG2 J190411+3627	BCU II	16.335	2.098	0.768	0.551	1.382	0.20	0.40	0.05	
J0017.2-0643	PMN J0017-0650	BCU II	13.67	2.116	0.770	–	–	0.17	–	–	
J1858.4-2509	PMN J1858-2511	BCU II	12.55	2.288	0.761	–	–	-0.02	–	–	
J0137.8+5813	1RXS J013748.0+581422	BCU II	16.58	2.057	0.753	0.512	–	0.39	0.55	–	
J0804.4+0418	MG1 J080357+0420	BCU II	12.875	2.566	0.834	–	–	-0.88	–	–	
J1949.0+1312	87GB 194635.4+130713	BCU II	15.45	2.162	0.764	–	–	0.15	–	–	
J0805.0-0622	1RXS J080458.3-062432	BCU II	16.25	1.895	0.706	0.464	0.732	0.85	0.85	0.75	
J0807.1+7744	NVSS J080637+774607	BCU II	12.527	2.436	0.812	–	–	-0.65	–	–	

Table 1—Continued

LAT Name	Counterpart Name	Class	$\log \nu_s$	$\Gamma_\gamma$	$\alpha_{r\gamma}$	$\alpha_{rx}$	$\alpha_{ox}$	$\rho_s^1$	$\rho_s^2$	$\rho_s^3$	IT
J0232.9+2606	B2 0230+25	BCU II	14.6	2.086	0.782	–	–	0.12	–	–	
J1841.2+2910	MG3 J184126+2910	BCU II	16.195	1.567	0.737	0.476	0.698	0.84	0.95	0.49	
J0223.3+6820	NVSS J022304+682154	BCU II	15.8	1.915	0.702	–	–	0.84	–	–	
J1830.0-4439	PMN J1830-4441	BCU II	12.62	2.217	0.778	–	–	-0.06	–	–	
J0813.3+6509	GB6 J0812+6508	BCU II	16.25	2.197	0.752	–	–	0.20	–	–	B
J0228.7-3106	PMN J0228-3102	BCU II	14.2	2.140	0.791	0.709	0.971	-0.04	-0.22	-0.26	
J1340.6-0408	NVSS J134042-041006	BCU II	15.344	1.981	0.724	–	–	0.70	–	–	B
J0228.0+2248	NVSS J022744+224834	BCU II	13.39	2.121	0.735	–	–	0.45	–	–	
J0250.6+5630	NVSS J025047+562935	BCU II	16.138	1.990	0.717	0.534	–	0.74	0.59	–	
J1933.4+0727	1RXS J193320.3+072616	BCU II	15.98	1.743	0.749	0.555	–	0.73	0.75	–	
J0302.0+5335	GB6 J0302+5331	BCU II	15.988	2.378	0.790	–	–	-0.39	–	–	
J0225.2-2602	PMN J0225-2603	BCU II	13.72	2.663	0.779	–	–	-0.55	–	–	
J0224.1-7941	PMN J0223-7940	BCU II	15.8	2.229	0.758	–	–	0.08	–	–	
J0019.1-5645	PMN J0019-5641	BCU II	12.83	2.391	0.775	–	–	-0.29	–	–	
J0304.9+6817	TXS 0259+681	BCU II	12.725	2.844	0.846	–	–	-0.95	–	–	
J0332.0+6308	GB6 J0331+6307	BCU II	14.15	2.331	0.729	–	–	0.14	–	–	
J1757.4+6536	7C 1757+6536	BCU II	14.195	2.317	0.768	–	–	-0.13	–	–	
J0219.0+2440	87GB 021610.9+243205	BCU II	15.8	1.857	0.747	–	–	0.68	–	–	B
J0218.9+3642	MG3 J021846+3641	BCU II	13.12	2.576	0.765	–	–	-0.39	–	–	
J0352.9+5655	GB6 J0353+5654	BCU II	16.315	1.833	0.734	–	–	0.80	–	–	B
J1747.1+0139	PMN J1746+0141	BCU II	12.9	2.643	0.763	–	–	-0.42	–	–	
J0842.0-6055	PMN J0842-6053	BCU II	13.355	2.328	0.810	–	–	-0.47	–	–	
J0425.2+6319	1RXS J042523.0+632016	BCU II	16.05	1.964	0.712	0.502	–	0.78	0.71	–	
J0444.5+3425	B2 0441+34	BCU II	13.005	2.183	0.793	–	–	-0.12	–	–	
J0216.6-1019	PMN J0216-1017	BCU II	12.655	2.329	0.816	–	–	-0.51	–	–	
J1106.4-3643	PMN J1106-3647	BCU II	13.81	2.292	0.737	–	–	0.13	–	–	
J0214.7-5823	PMN J0214-5822	BCU II	13.705	2.570	0.807	–	–	-0.71	–	–	
J0213.1-2720	PMN J0212-2719	BCU II	13.81	2.089	0.770	–	–	0.20	–	–	
J0501.8+3046	1RXS J050140.8+304831	BCU II	16.1	2.124	0.729	0.502	–	0.48	0.48	–	
J0858.1-1951	PKS 0855-19	BCU II	13.502	2.463	0.840	0.765	0.859	-0.82	-0.79	-0.69	
J0211.2-0649	NVSS J021116-064422	BCU II	14.6	2.099	0.735	–	–	0.49	–	–	
J0503.4+4522	1RXS J050339.8+451715	BCU II	15.645	2.360	0.723	0.492	–	0.14	0.18	–	
J1208.2-7810	PKS 1205-778	BCU II	14.03	2.146	0.802	–	–	-0.12	–	–	
J0904.3+4240	S4 0900+42	BCU II	12.572	2.476	0.862	–	–	-0.84	–	–	Q
J0512.9+4038	B3 0509+406	BCU II	13.635	2.100	0.819	–	–	-0.16	–	–	
J1656.8-2010	1RXS J165655.0-201049	BCU II	16.065	1.961	0.707	0.498	0.655	0.79	0.72	0.69	B
J1656.0+2044	MG2 J165546+2043	BCU II	12.27	2.493	0.721	–	–	-0.02	–	–	
J1207.6-2232	NVSS J120738-223250	BCU II	12.62	2.575	0.767	–	–	-0.41	–	–	
J0956.7-6441	AT20G J095612-643928	BCU II	13.285	2.536	0.770	–	–	-0.40	–	–	
J1647.1-6438	PMN J1647-6437	BCU II	13.495	2.189	0.819	–	–	-0.30	–	–	
J1924.9+2817	NVSS J192502+281542	BCU II	15.85	1.884	0.748	0.525	–	0.64	0.74	–	
J1643.6-0642	NVSS J164328-064619	BCU II	17	2.071	0.713	0.532	1.095	0.64	0.49	0.61	
J0204.2+2420	B2 0201+24	BCU II	14.446	1.792	0.793	–	–	0.35	–	–	
J1912.0-0804	PMN J1912-0804	BCU II	15.05	2.295	0.799	0.716	–	-0.34	-0.49	–	
J0915.0+5844	SDSS J091608.57+584434.0	BCU II	13.92	2.482	0.868	–	–	-0.84	–	–	
J0620.4+2644	RX J0620.6+2644	BCU II	16.085	1.650	0.758	0.482	–	0.70	0.95	–	



Table 1—Continued

LAT Name	Counterpart Name	Class	$\log \nu_s$	$\Gamma_\gamma$	$\alpha_{r\gamma}$	$\alpha_{rx}$	$\alpha_{ox}$	$\rho_s^1$	$\rho_s^2$	$\rho_s^3$	IT
J0203.1-0227	RX J0202.9-0223	BCU II	16.4	2.313	0.777	0.595	–	-0.21	0.00	–	
J0622.9+3326	B2 0619+33	BCU II	14.05	2.095	0.709	–	–	0.62	–	–	
J0623.3+3043	GB6 J0623+3045	BCU II	14.79	1.893	0.745	–	–	0.66	–	–	
J0200.9-6635	PMN J0201-6638	BCU II	12.515	2.331	0.800	0.732	0.812	-0.41	-0.60	-0.30	
J0631.2+2019	TXS 0628+203	BCU II	15	2.460	0.802	–	–	-0.59	–	–	
J0640.0-1252	TXS 0637-128	BCU II	16.05	1.512	0.777	0.515	–	0.61	0.87	–	
J1910.8+2855	1RXS J191053.2+285622	BCU II	16.91	1.464	0.674	0.378	–	0.98	0.99	–	
J1908.8-0130	NVSS J190836-012642	BCU II	11.782	2.148	0.716	–	–	0.51	–	–	
J1617.3-2519	PMN J1617-2537	BCU II	12.483	2.591	0.773	–	–	-0.47	–	–	
J0156.9-4742	2MASS J01564603-4744174	BCU II	15.35	2.009	0.754	–	–	0.45	–	–	B
J0156.3+3913	MG4 J015630+3913	BCU II	13.2	2.495	0.786	–	–	-0.50	–	–	
J0650.4-1636	PKS 0648-16	BCU II	11.465	2.433	0.846	–	–	-0.79	–	–	
J0650.5+2055	1RXS J065033.9+205603	BCU II	15.65	1.558	0.665	0.481	–	0.98	0.94	–	
J0747.2-3311	PKS 0745-330	BCU II	13.85	2.309	0.778	–	–	-0.21	–	–	
J0658.6+0636	NVSS J065844+063711	BCU II	15	2.481	0.733	–	–	-0.07	–	–	
J0031.3+0724	NVSS J003119+072456	BCU II	15.176	1.824	0.713	–	–	0.89	–	–	
J0700.0+1709	TXS 0657+172	BCU II	12.725	2.687	0.835	–	–	-0.93	–	–	Q
J1315.4+1130	1RXS J131531.9+113327	BCU II	16.525	1.962	0.731	0.514	0.702	0.68	0.68	0.55	B
J0151.0+0537	PMN J0151+0540	BCU II	13.74	2.359	0.809	–	–	-0.52	–	–	
J0150.5-5447	PMN J0150-5450	BCU II	15.552	2.118	0.766	–	–	0.20	–	–	
J0700.2+1304	GB6 J0700+1304	BCU II	15.425	1.805	0.756	–	–	0.63	–	–	B
J1156.7-2250	NVSS J115633-225004	BCU II	15.4	1.890	0.713	–	–	0.85	–	–	
J0146.4-6746	SUMSS J014554-674646	BCU II	14.958	2.391	0.756	–	–	-0.13	–	–	
J1549.7-0658	NVSS J154952-065907	BCU II	17.35	1.924	0.675	–	–	0.84	–	–	
J0953.1-7657	1RXS J095306.1-765755	BCU II	14.919	1.912	0.714	0.537	0.812	0.82	0.68	0.75	
J1549.5+1709	MG1 J154930+1708	BCU II	13.425	1.916	0.771	–	–	0.41	–	–	B
J1549.0+6309	SDSS J154958.45+631021.2	BCU II	13.432	2.726	0.803	–	–	-0.76	–	–	
J1314.7-4237	MS 13121-4221	BCU II	16.28	2.082	0.714	–	–	0.62	–	–	
J0139.9+8735	NVSS J013913+873754	BCU II	14.1	1.891	0.704	–	–	0.86	–	–	
J0043.5-0444	1RXS J004333.7-044257	BCU II	17.25	1.735	0.736	0.506	0.587	0.83	0.88	0.46	B
J0030.2-1646	1RXS J003019.6-164723	BCU II	15.52	1.647	0.686	0.529	1.074	0.97	0.85	0.75	B
J0958.6-2447	TXS 0956-244	BCU II	13.915	2.242	0.790	–	–	-0.19	–	–	
J1525.2-5905	PMN J1524-5903	BCU II	12.655	2.787	0.809	–	–	-0.82	–	–	
J1508.7-4956	PMN J1508-4953	BCU II	11.78	2.731	0.829	0.763	–	-0.90	-0.87	–	
J0133.3+4324	B3 0129+431	BCU II	13.48	2.301	0.796	–	–	-0.32	–	–	
J0051.2-6241	1RXS J005117.7-624154	BCU II	15.904	1.663	0.694	0.529	0.982	0.97	0.84	0.82	
J0746.6-0706	PMN J0746-0709	BCU II	14.23	2.191	0.752	–	–	0.21	–	–	
J1419.1-5156	PMN J1419-5155	BCU II	12.55	2.662	0.835	–	–	-0.94	–	–	
J1400.7-5605	PMN J1400-5605	BCU II	12.28	2.497	0.763	–	–	-0.32	–	–	
J1823.6-3453	NVSS J182338-345412	BCU II	16.14	1.748	0.720	0.441	–	0.91	0.95	–	
J1008.9-2910	PMN J1008-2912	BCU II	12.68	2.391	0.777	–	–	-0.31	–	–	
J0804.0-3629	NVSS J080405-362919	BCU II	15.92	1.829	0.719	–	–	0.88	–	–	
J0127.2+0325	NVSS J012713+032259	BCU II	15.95	1.899	0.682	–	–	0.87	–	–	
J0816.7-2421	PMN J0816-2421	BCU II	12.34	2.432	0.781	–	–	-0.39	–	–	
J0825.8-3217	PKS 0823-321	BCU II	14.03	2.490	0.801	–	–	-0.62	–	–	
J1016.1+5555	TXS 1012+560	BCU II	14.125	2.525	0.797	–	–	-0.61	–	–	Q

Table 1—Continued

LAT Name	Counterpart Name	Class	$\log \nu_s$	$\Gamma_\gamma$	$\alpha_{r\gamma}$	$\alpha_{rx}$	$\alpha_{ox}$	$\rho_s^1$	$\rho_s^2$	$\rho_s^3$	IT
J1018.1+1904	MG1 J101810+1903	BCU II	14.02	1.984	0.747	–	–	0.55	–	–	
J1434.6+6640	1RXS J143442.0+664031	BCU II	15.379	1.517	0.706	0.568	–	0.97	0.78	–	B
J0845.1-5458	PMN J0845-5458	BCU II	13.005	2.295	0.799	0.776	–	-0.33	-0.66	–	B
J1022.3-4234	PMN J1022-4232	BCU II	13.705	2.336	0.783	–	–	-0.28	–	–	
J0849.5-2912	NVSS J084922-291149	BCU II	14.504	2.118	0.705	–	–	0.60	–	–	
J0849.9-3540	PMN J0849-3541	BCU II	12.9	2.371	0.789	–	–	-0.37	–	–	
J1322.3+0839	NVSS J132210+084231	BCU II	13.16	2.253	0.760	–	–	0.02	–	–	Q
J0853.0-3654	NVSS J085310-365820	BCU II	15.66	2.059	0.765	–	–	0.29	–	–	
J0858.1-3130	1RXS J085802.6-313043	BCU II	16.235	1.731	0.679	0.375	–	0.94	0.96	–	
J1026.5+7423	GB6 J1027+7428	BCU II	13.53	2.573	0.811	–	–	-0.75	–	–	
J0904.8-3516	NVSS J090442-351423	BCU II	14.171	2.651	0.787	–	–	-0.59	–	–	
J1322.6-1619	PMN J1322-1617	BCU II	13.67	2.356	0.785	–	–	-0.32	–	–	
J0922.8-3959	PKS 0920-39	BCU II	13.775	2.702	0.886	0.799	–	-0.96	-0.92	–	
J1322.8-0938	PMN J1323-0943	BCU II	12.6	2.629	0.803	–	–	-0.72	–	–	
J1659.7-3132	NVSS J165949-313047	BCU II	13.11	2.402	0.784	–	–	-0.38	–	–	
J1005.0-4959	PMN J1006-5018	BCU II	12.14	2.777	0.869	–	–	-0.99	–	–	
J0113.0-3554	PMN J0112-3552	BCU II	12.69	2.503	0.782	–	–	-0.48	–	–	
J1015.2-4512	PMN J1014-4508	BCU II	12.025	2.239	0.822	–	–	-0.40	–	–	
J0043.7-1117	1RXS J004349.3-111612	BCU II	15.44	1.594	0.722	0.575	1.015	0.90	0.75	0.62	
J1047.8-6216	PMN J1047-6217	BCU II	12.2	2.603	0.822	–	–	-0.85	–	–	
J1051.5-6517	PKS 1049-650	BCU II	14.03	2.596	0.781	–	–	-0.52	–	–	
J1049.8+1425	MG1 J104945+1429	BCU II	13.95	2.332	0.785	–	–	-0.29	–	–	
J1052.8-3741	PMN J1053-3743	BCU II	14.475	1.996	0.756	–	–	0.45	–	–	
J1440.0-3955	1RXS J143949.8-395524	BCU II	15.728	1.864	0.719	0.557	1.244	0.85	0.66	0.51	
J1419.5-0836	NVSS J141922-083830	BCU II	12.76	2.271	0.783	–	–	-0.18	–	–	
J0107.0-1208	PMN J0107-1211	BCU II	14.04	2.180	0.767	–	–	0.10	–	–	
J1233.9-5736	AT20G J123407-573552	BCU II	14.7	2.164	0.716	–	–	0.48	–	–	
J1424.6-6807	PKS 1420-679	BCU II	12.48	2.536	0.833	–	–	-0.86	–	–	
J1342.7+0945	NVSS J134240+094752	BCU II	14.36	1.870	0.731	–	–	0.80	–	–	
J1304.3-5535	PMN J1303-5540	BCU II	12.725	2.696	0.840	–	–	-0.95	–	–	
J1308.1-6707	PKS 1304-668	BCU II	14.23	2.450	0.791	–	–	-0.48	–	–	
J1323.0+2942	4C 29.48	BCU II	13.4	2.145	0.820	0.845	–	-0.24	-0.55	–	
J1109.4-4815	PMN J1109-4815	BCU II	12.97	2.494	0.816	–	–	-0.73	–	–	
J1345.9-3357	NVSS J134543-335643	BCU II	14.2	2.466	0.753	–	–	-0.20	–	–	
J1328.5-4728	1WGA J1328.6-4727	BCU II	15.645	1.699	0.739	–	–	0.81	–	–	B
J0049.4-5401	PMN J0049-5402	BCU II	15.56	2.143	0.803	–	–	-0.12	–	–	
J1711.5-5029	PMN J1711-5028	BCU II	13.39	2.558	0.778	–	–	-0.49	–	–	
J0211.7+5402	TXS 0207+538	BCU III	–	2.691	0.836	–	–	-0.94	–	–	
J0039.1+4330	NVSS J003907+433015	BCU III	–	1.963	0.694	–	–	0.81	–	–	
J2108.6-8619	1RXS J210959.5-861853	BCU III	–	1.740	0.735	0.624	1.043	0.83	0.52	0.48	
J0733.5+5153	NVSS J073326+515355	BCU III	–	1.741	0.727	–	–	0.89	–	–	
J1218.5+6912	NVSS J122044+690522	BCU III	–	3.019	0.755	0.433	0.516	-0.51	-0.21	0.26	
J0217.3+6209	TXS 0213+619	BCU III	–	2.726	0.748	–	–	-0.34	–	–	
J1848.1-4230	PMN J1848-4230	BCU III	–	1.951	0.763	–	–	0.44	–	–	
J1711.6+8846	1RXS J171643.8+884414	BCU III	–	1.570	0.704	0.516	–	0.97	0.88	–	
J0223.5+6313	TXS 0219+628	BCU III	–	2.776	0.760	–	–	-0.46	–	–	

Table 1—Continued

LAT Name	Counterpart Name	Class	$\log \nu_s$	$\Gamma_\gamma$	$\alpha_{r\gamma}$	$\alpha_{rx}$	$\alpha_{ox}$	$\rho_s^1$	$\rho_s^2$	$\rho_s^3$	IT
J0519.3+2746	4C 27.15	BCU III	–	2.330	0.858	–	–	-0.67	–	–	
J0135.0+6927	TXS 0130+691	BCU III	–	2.557	0.804	–	–	-0.67	–	–	
J0244.4-8224	PMN J0251-8226	BCU III	–	2.679	0.787	0.608	0.941	-0.61	-0.43	-0.21	
J0418.0-0251	PKS B0415-029	BCU III	–	2.461	0.757	–	–	-0.22	–	–	
J0509.7-6418	RBS 625	BCU III	–	2.000	0.724	0.489	–	0.68	0.68	–	
J1835.4+1349	TXS 1833+137	BCU III	–	2.461	0.801	–	–	-0.59	–	–	B
J1831.0-2714	PMN J1831-2714	BCU III	–	2.211	0.770	–	–	0.01	–	–	
J0742.4-8133	SUMSS J074220-813139	BCU III	–	1.464	0.726	–	–	0.89	–	–	
J1939.6-4925	SUMSS J193946-492539	BCU III	–	1.624	0.692	–	–	0.97	–	–	
J1741.9-2539	NVSS J174154-253743	BCU III	–	2.206	0.714	–	–	0.43	–	–	
J2213.6-4755	SUMSS J221330-475426	BCU III	–	1.889	0.737	–	–	0.74	–	–	
J0228.5+6703	GB6 J0229+6706	BCU III	–	2.619	0.741	–	–	-0.24	–	–	
J1949.4-6140	PMN J1949-6137	BCU III	–	2.308	0.810	–	–	-0.44	–	–	
J0525.8-2014	PMN J0525-2010	BCU III	–	2.063	0.801	–	–	0.02	–	–	
J0358.7+0633	PMN J0358+0629	BCU III	–	2.633	0.727	–	–	-0.16	–	–	
J0723.2-0728	1RXS J072259.5-073131	BCU III	–	1.798	0.763	0.502	–	0.58	0.86	–	B
J2353.7-3911	NVSS J235342-391442	BCU III	–	2.281	0.714	–	–	0.30	–	–	
J2353.3-4805	SUMSS J235310-480558	BCU III	–	2.010	0.780	–	–	0.22	–	–	
J0830.3-5855	PMN J0829-5856	BCU III	–	2.608	0.750	–	–	-0.29	–	–	
J2107.7-4822	PMN J2107-4827	BCU III	–	2.711	0.778	–	–	-0.56	–	–	
J0542.2-8737	SUMSS J054923-874001	BCU III	–	2.039	0.731	–	–	0.59	–	–	
J0542.5-0907	PMN J0542-0913	BCU III	–	2.567	0.795	–	–	-0.61	–	–	
J0343.3-6443	PMN J0343-6442	BCU III	–	2.154	0.756	–	–	0.24	–	–	
J0121.7+5154	NVSS J012133+515557	BCU III	–	1.984	0.687	–	–	0.80	–	–	
J0103.7+1323	NVSS J010345+132346	BCU III	–	1.984	0.747	–	–	0.54	–	–	B
J1229.8-5305	AT20G J122939-530332	BCU III	–	2.147	0.758	–	–	0.24	–	–	
J0627.9-1517	NVSS J062753-152003	BCU III	–	2.724	0.775	0.534	–	-0.55	-0.26	–	
J0626.6-4259	1RXS J062635.9-425810	BCU III	–	1.740	0.701	0.563	1.056	0.96	0.73	0.70	
J0434.0-5726	SUMSS J043344-572613	BCU III	–	1.999	0.701	–	–	0.76	–	–	
J0825.4-0213	PMN J0825-0204	BCU III	–	2.401	0.793	–	–	-0.44	–	–	
J0453.2+6321	NVSS J045312+632117	BCU III	–	2.347	0.713	–	–	0.22	–	–	
J1258.7+5137	NVSS J125825+514225	BCU III	–	2.159	0.769	–	–	0.10	–	–	
J1207.6-4537	PMN J1207-4531	BCU III	–	2.113	0.788	–	–	0.03	–	–	
J1925.7+1228	TXS 1923+123	BCU III	–	2.606	0.760	–	–	-0.37	–	–	
J1310.6+2446	MG2 J131037+2447	BCU III	–	2.202	0.796	–	–	-0.17	–	–	
J1849.3-1645	1RXS J184919.7-164726	BCU III	–	1.606	0.719	0.516	–	0.92	0.88	–	
J1822.1-7051	PMN J1823-7056	BCU III	–	2.703	0.869	–	–	-0.97	–	–	
J1312.7-2349	NVSS J131248-235046	BCU III	–	1.801	0.708	–	–	0.92	–	–	
J0028.8+1951	TXS 0025+197	BCU III	–	2.434	0.815	–	–	-0.67	–	–	Q
J0515.5-0123	NVSS J051536-012427	BCU III	–	1.755	0.774	–	–	0.51	–	–	
J0409.4+3158	NVSS J040928+320245	BCU III	–	2.373	0.714	0.404	0.447	0.18	0.32	0.52	
J1153.7-2555	PMN J1153-2553	BCU III	–	2.015	0.777	–	–	0.25	–	–	
J1744.9-1725	1RXS J174459.5-172640	BCU III	–	2.076	0.694	0.436	–	0.70	0.64	–	
J0354.1+4643	B3 0350+465	BCU III	–	2.380	0.833	–	–	-0.68	–	–	
J1718.1-3056	PMN J1718-3056	BCU III	–	2.374	0.758	–	–	-0.11	–	–	
J1739.0+8716	NVSS J173722+871744	BCU III	–	2.277	0.749	–	–	0.07	–	–	

Table 1—Continued

LAT Name	Counterpart Name	Class	$\log \nu_s$	$\Gamma_\gamma$	$\alpha_{r\gamma}$	$\alpha_{rx}$	$\alpha_{ox}$	$\rho_s^1$	$\rho_s^2$	$\rho_s^3$	IT
J0525.6-6013	SUMSS J052542-601341	BCU III	–	1.726	0.696	0.570	0.759	0.96	0.71	0.81	
J1648.5-4829	PMN J1648-4826	BCU III	–	2.438	0.788	–	–	-0.45	–	–	
J1645.2-5747	AT20G J164513-575122	BCU III	–	2.675	0.804	–	–	-0.75	–	–	
J1600.3-5810	MRC 1556-580	BCU III	–	2.008	0.806	–	–	0.05	–	–	
J2312.9-6923	SUMSS J231347-692332	BCU III	–	1.804	0.717	0.522	0.725	0.90	0.81	0.67	
J1256.1-5919	PMN J1256-5919	BCU III	–	2.293	0.741	–	–	0.11	–	–	
J1101.5+4106	B3 1058+413	BCU III	–	1.768	0.795	–	–	0.35	–	–	
J2041.9-7318	SUMSS J204201-731911	BCU III	–	2.210	0.738	–	–	0.28	–	–	
J0502.7+3438	MG2 J050234+3436	BCU III	–	2.286	0.768	–	–	-0.08	–	–	
J1123.2-6415	AT20G J112319-641735	BCU III	–	2.241	0.772	–	–	-0.05	–	–	
J1451.2+6355	TXS 1450+641	BCU III	–	1.881	0.823	–	–	0.08	–	–	
J0512.2+2918	B2 0509+29	BCU III	–	2.569	0.803	0.656	–	-0.68	-0.51	–	
J1855.1-6008	PMN J1854-6009	BCU III	–	1.813	0.777	–	–	0.46	–	–	
J0116.2-2744	1RXS J011555.6-274428	BCU III	–	2.022	0.725	0.521	0.658	0.64	0.58	0.58	
J0148.3+5200	GB6 J0148+5202	BCU III	–	1.770	0.724	–	–	0.89	–	–	B
J2336.5-7620	PMN J2336-7620	BCU III	–	2.330	0.786	–	–	-0.30	–	–	
J0828.8-2420	NVSS J082841-241850	BCU III	–	2.000	0.797	–	–	0.14	–	–	B
J0528.3+1815	1RXS J052829.6+181657	BCU III	–	1.646	0.722	0.425	–	0.91	0.98	–	
J0744.1-3804	PMN J0743-3804	BCU III	–	2.680	0.813	–	–	-0.81	–	–	
J1955.9+0212	NVSS J195547+021514	BCU III	–	1.927	0.725	0.501	1.176	0.77	0.75	0.50	
J0611.7+2759	GB6 J0611+2803	BCU III	–	2.277	0.719	–	–	0.28	–	–	
J1559.8-2525	NVSS J160005-252439	BCU III	–	1.944	0.750	–	–	0.57	–	–	
J1030.4-2030	NVSS J103040-203032	BCU III	–	1.889	0.682	0.569	1.075	0.87	0.60	0.76	
J0145.6+8600	NVSS J014929+860114	BCU III	–	2.519	0.795	–	–	-0.58	–	–	
J1504.5-8242	1RXS J150537.1-824233	BCU III	–	2.298	0.754	0.532	0.547	0.02	0.19	0.27	
J1146.8+3958	NVSS J114653+395751	BCU III	–	2.321	0.670	–	–	0.42	–	–	
J1158.9+0818	RX J1158.8+0819	BCU III	–	1.869	0.699	0.524	–	0.88	0.76	–	
J0521.9-3847	PKS 0520-388	BCU III	–	2.627	0.817	–	–	-0.83	–	–	
J1136.6-6826	PKS 1133-681	BCU III	–	2.711	0.828	–	–	-0.90	–	–	
J1537.8-8000	PMN J1537-7958	BCU III	–	2.186	0.736	–	–	0.33	–	–	
J1511.8-0513	NVSS J151148-051345	BCU III	–	2.034	0.688	–	–	0.75	–	–	B

Note. —  $\rho_s^1, \rho_s^2, \rho_s^3$  are the likelihood  $\rho_s$  values in the  $z$ -score  $\tilde{\Gamma}_\gamma-\tilde{\alpha}_{r\gamma}, \tilde{\Gamma}_\gamma-\tilde{\alpha}_{rx}, \tilde{\alpha}_{ox}-\tilde{\alpha}_{r\gamma}$  planes, respectively.

Note. — “IT” indicates the identified blazar types reported in Massaro et al. (2016, reference therein) by optical spectroscopic observations, where “B” and “Q” indicate BL Lac and FSRQ, respectively.

Table 2. Summary of Classification for BCUs with the Selected Spectral Planes

Spectral Plane	Type	Sources	FSRQ-like	BL Lac-like
$\tilde{\Gamma}_\gamma - \tilde{\alpha}_{r\gamma}$	BCU I	68	19	15
	BCU II	429	82	153
	BCU III	86	13	33
	All	583	114	201
$\tilde{\Gamma}_\gamma - \tilde{\alpha}_{rx}$	BCU I	33	3	21
	BCU II	123	9	99
	BCU III	20	0	16
	All	176	12	136
$\tilde{\alpha}_{ox} - \tilde{\alpha}_{r\gamma}$	BCU I	28	4	8
	BCU II	85	5	59
	BCU III	11	0	10
	All	124	9	77

Table 3. Comparison of our Results with Spectroscopic Identification for a Sample of 78 BCUs Taken from Massaro et al. (2016)

Test sample	Class <sup>a</sup>	$N^a$	Spectral Plane	$N_1^b/N$	$N_2^b/N$
Radio-selected	FSRQs	15	$\tilde{\Gamma}_\gamma - \tilde{\alpha}_{r\gamma}$	9/15	1/9
(78 sources)	BL Lacs	63		42/63	1/63
X-selected	FSRQs	3	$\tilde{\Gamma}_\gamma - \tilde{\alpha}_{rx}$	1/3	0/3
(34 sources)	BL Lacs	31		29/31	0/31
Optical-selected	FSRQs	3	$\tilde{\alpha}_{ox} - \tilde{\alpha}_{r\gamma}$	0/3	0/3
(28 sources)	BL Lacs	25		20/25	0/25

Note. — <sup>a</sup> Identified type with spectroscopic observation, and  $N$  is the source number of each type.

Note. — <sup>b</sup>  $N_1$  (or  $N_2$ ) is the number of sources that the evaluation with our method in given spectral planes within  $\sigma > 90\%$  is consistent (or inconsistent) with the classification by spectroscopic observations.

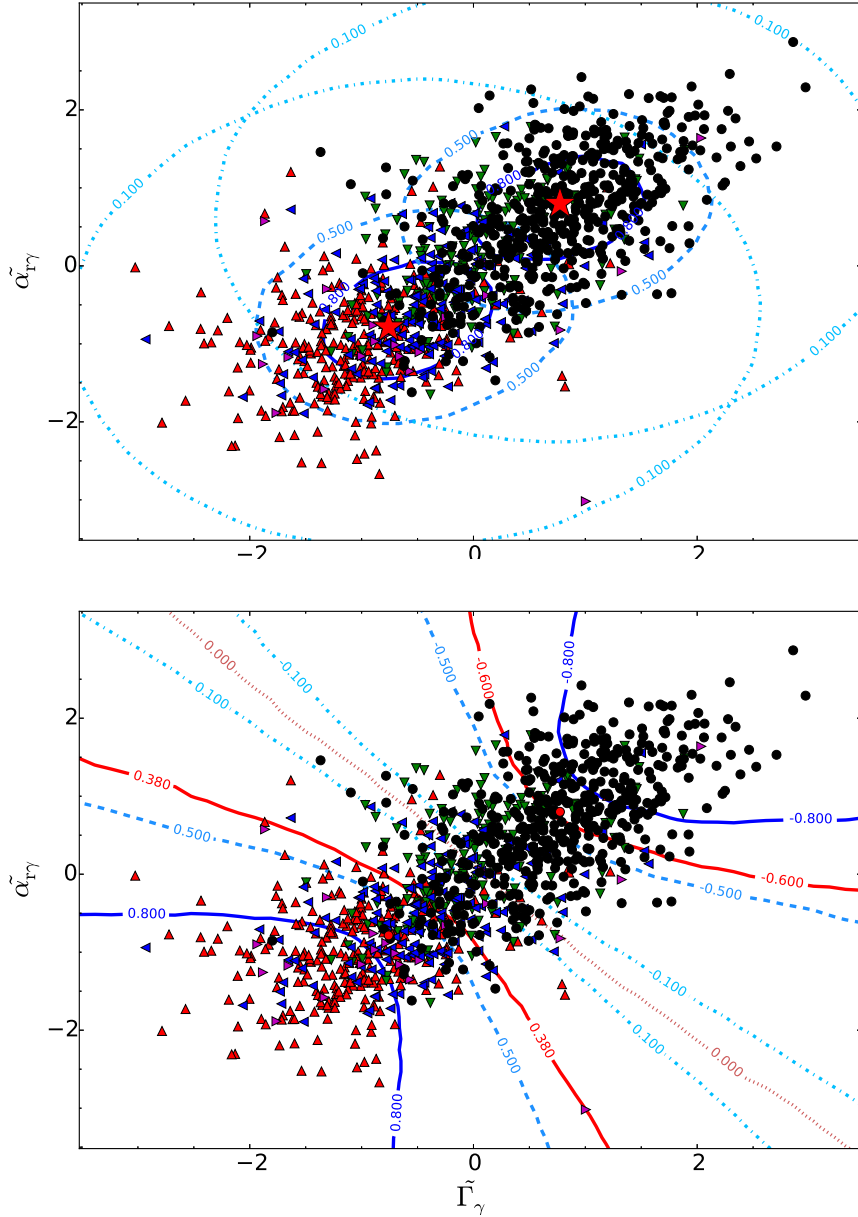
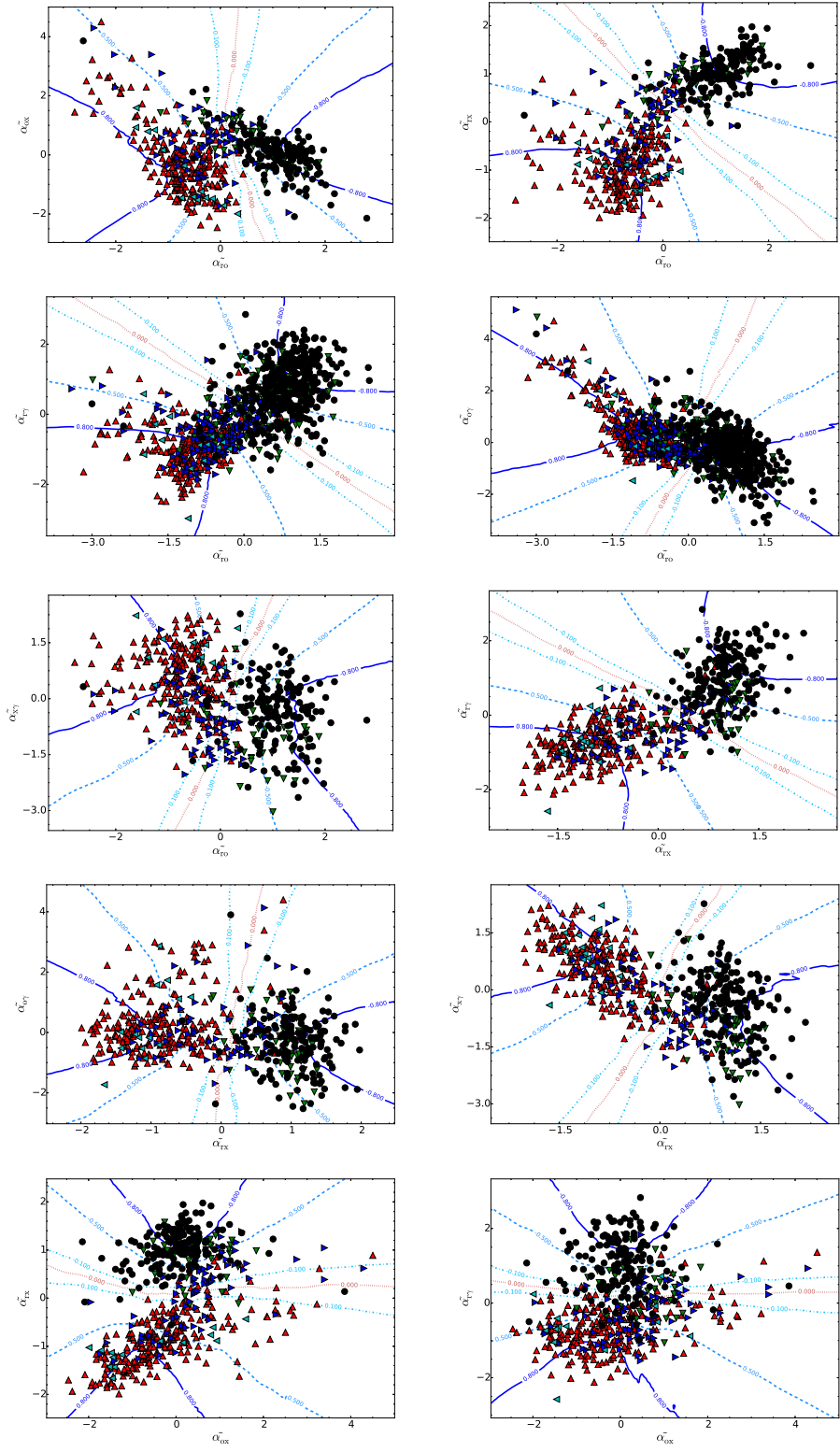


Fig. 1.— Distributions of the identified BL Lacs and FSRQs in 3LAC in the  $z$ -score  $\tilde{\Gamma}_{\gamma} - \tilde{\alpha}_{r\gamma}$  plane. The *black circles*, *red triangles*, *blue triangles*, *green triangles*, and *magenta triangles* stand for FSRQs, HSP-BL Lacs, ISP-BL Lacs, LSP-BL Lacs, and BL Lacs without  $\nu_s$  value available, respectively. The centroid points (*red stars*) and the  $p_{i,c}$  contours of FSRQs and BL Lacs are shown in the upper panel. The likelihood measurement  $\rho_s$  contours are shown in the lower panel.





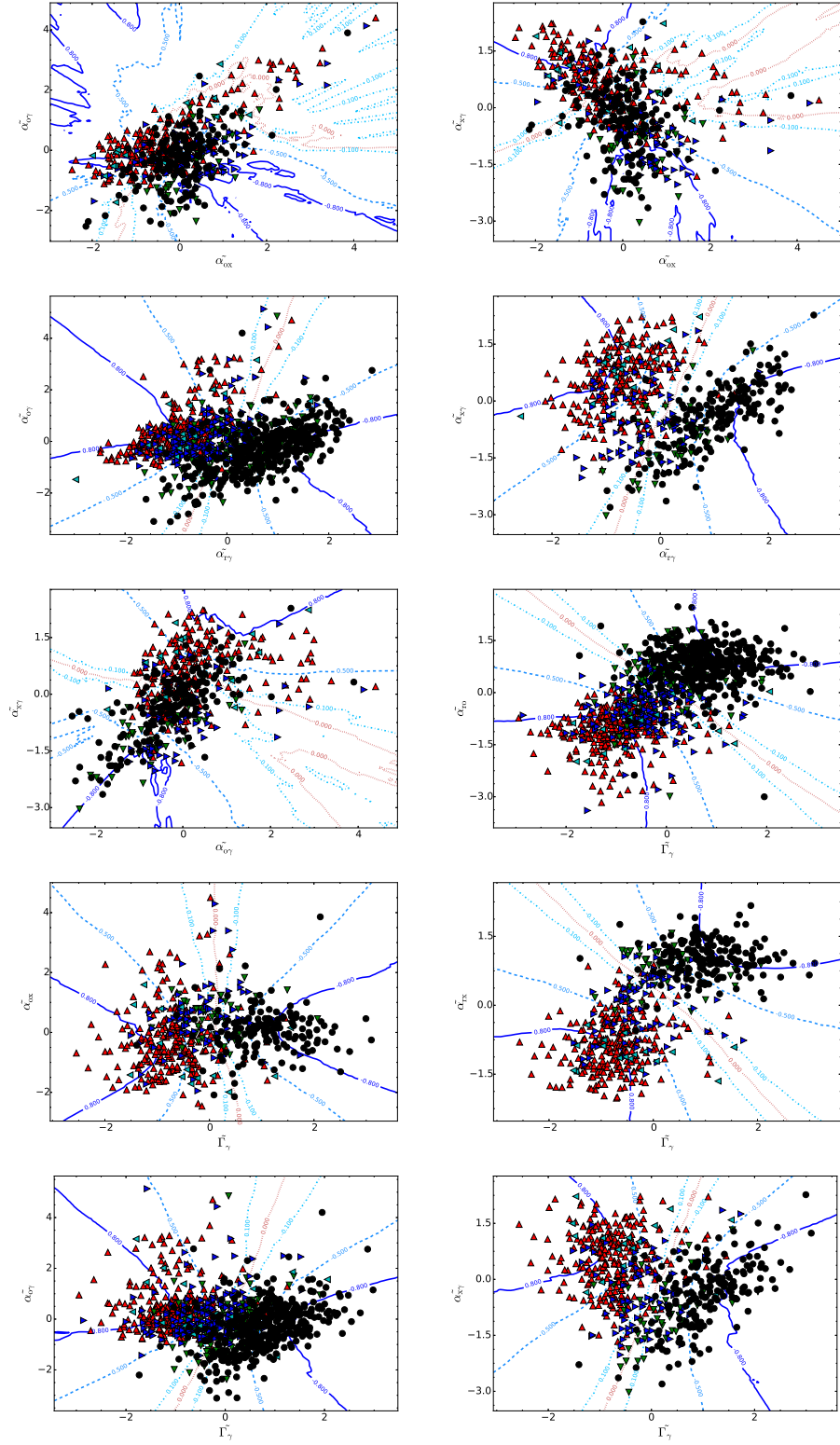
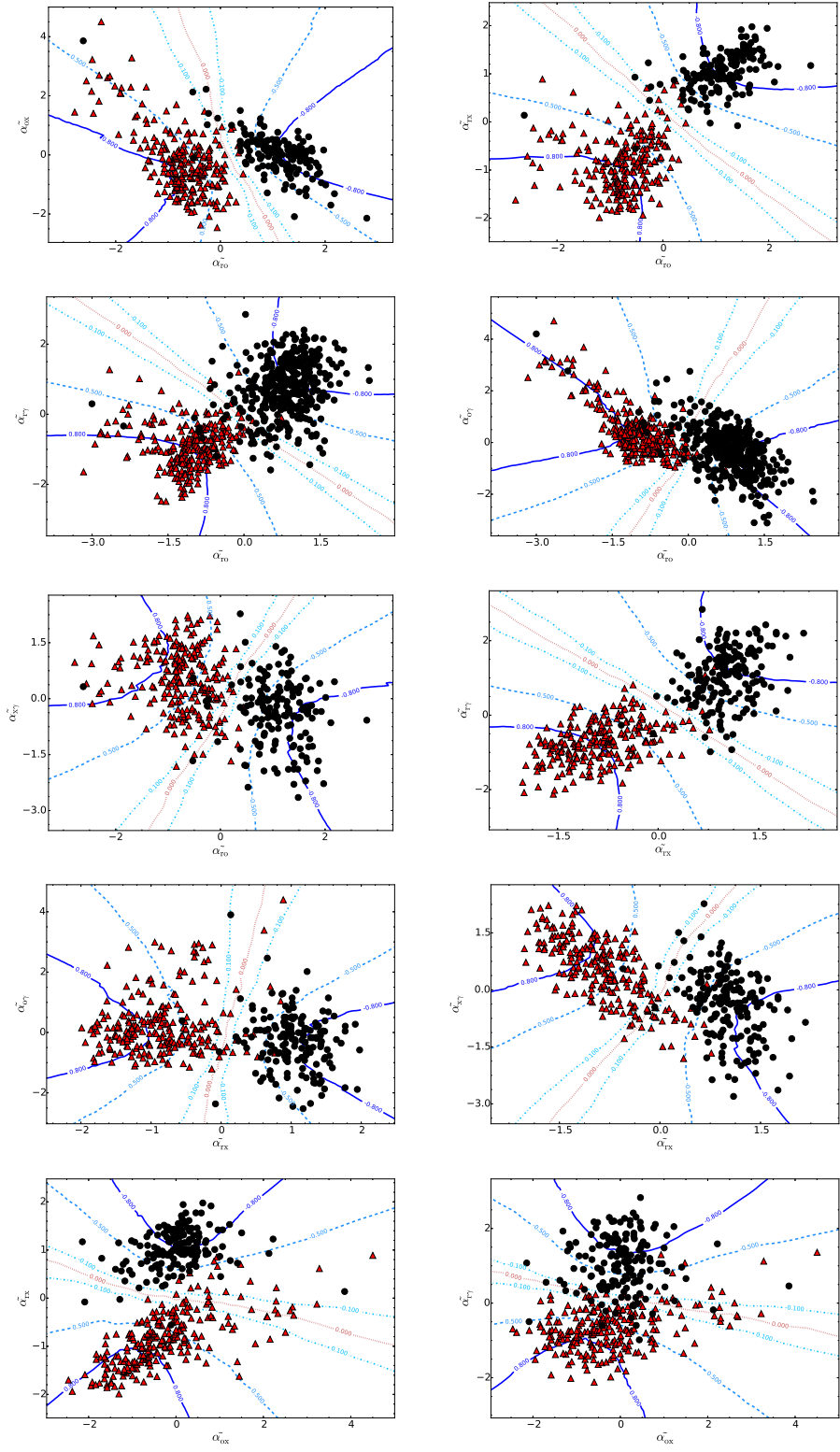


Fig. 2.— Distributions of the reference BL Lacs and FSRQs in the various  $z$ -score spectral planes with their corresponding  $\rho_s$  contours. The symbols are same as in Figure 1.



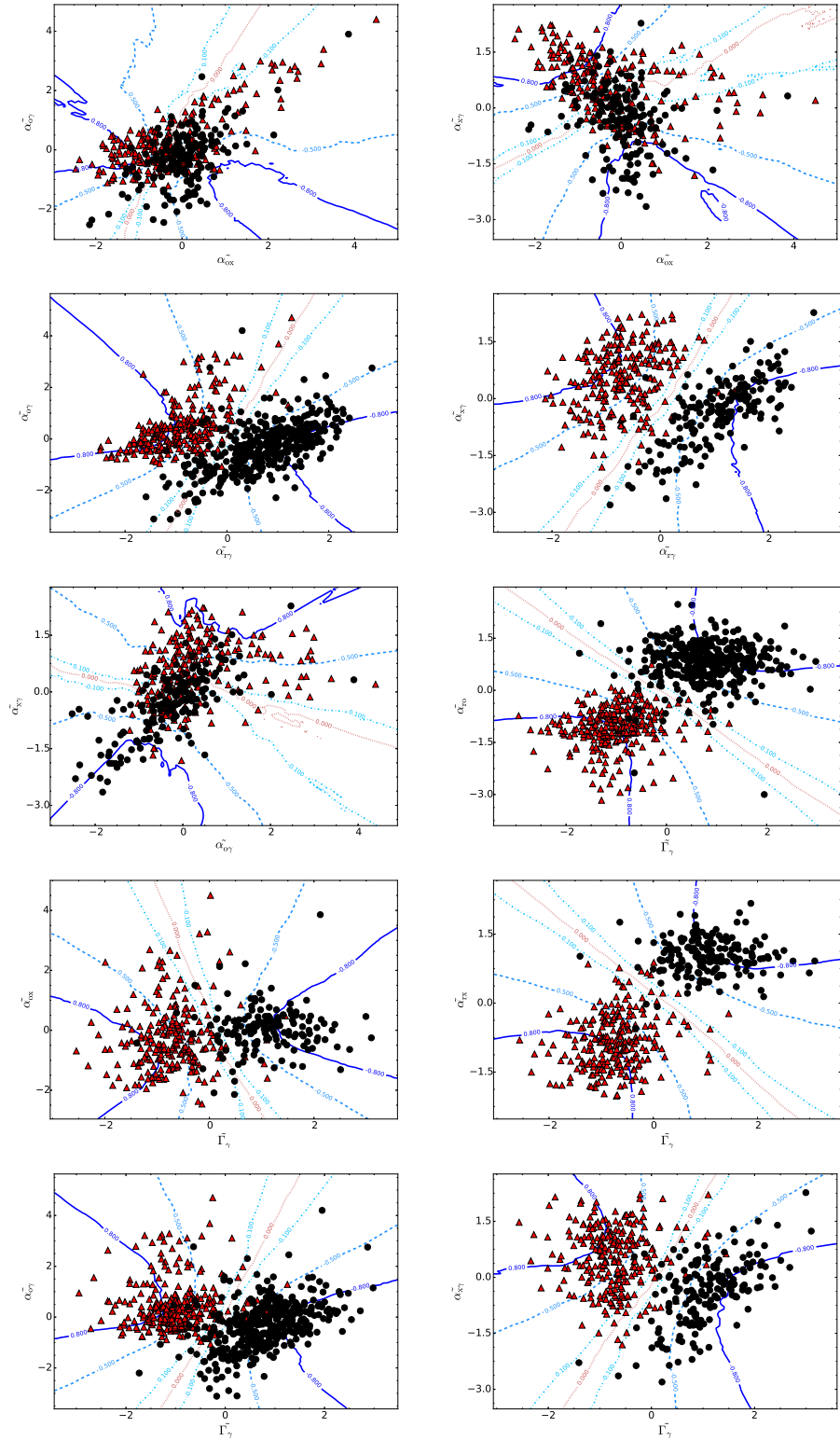


Fig. 3.— The same as Figure 2, but for the HSP-BL Lacs (*red triangles*) and FSRQs (*black circles*) only.

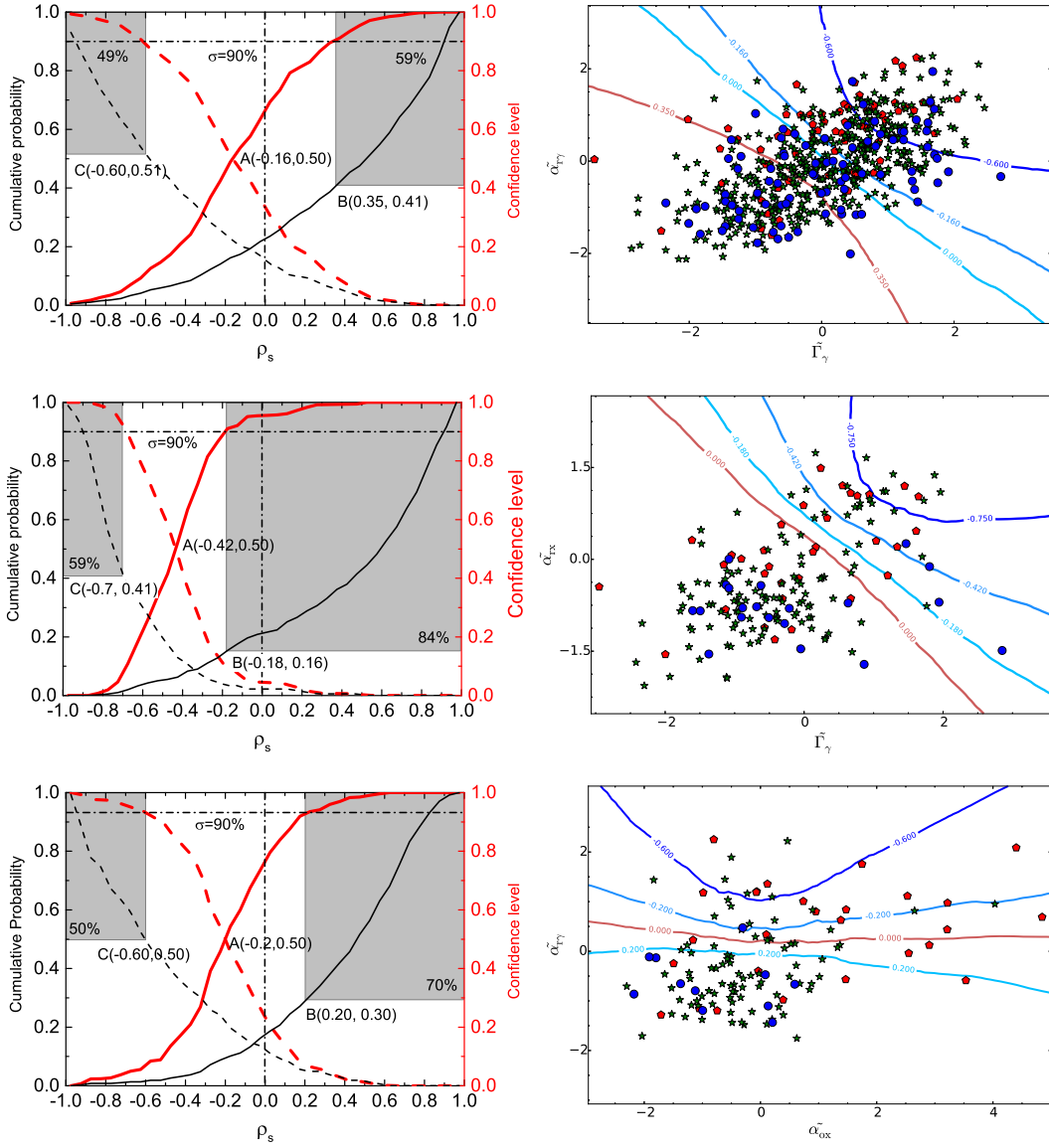


Fig. 4.— *Left panels:* the cumulative probabilities ( $P$ , black lines) and the confidence levels ( $\sigma$ , red lines) as a function of  $\rho_s$  derived from the current identified FSRQs (dashed lines) and BL Lacs (solid lines) observed with *Fermi*/LAT. Cross points “A” indicate a confidence level of 50% for classifying the two types of blazars. The shaded regions defined with cross points “B” and “C” indicate the percentages of sources and the  $\rho_s$  at a confidence level of 90%. *Right panels:* Distributions of BCUs together with the  $\rho_s$  contours derived from our reference samples in the corresponding planes. The *red pentagons*, *green stars*, and *blue circles* indicate BCU-Is, BCU-IIs, and BCU-IIIs, respectively.

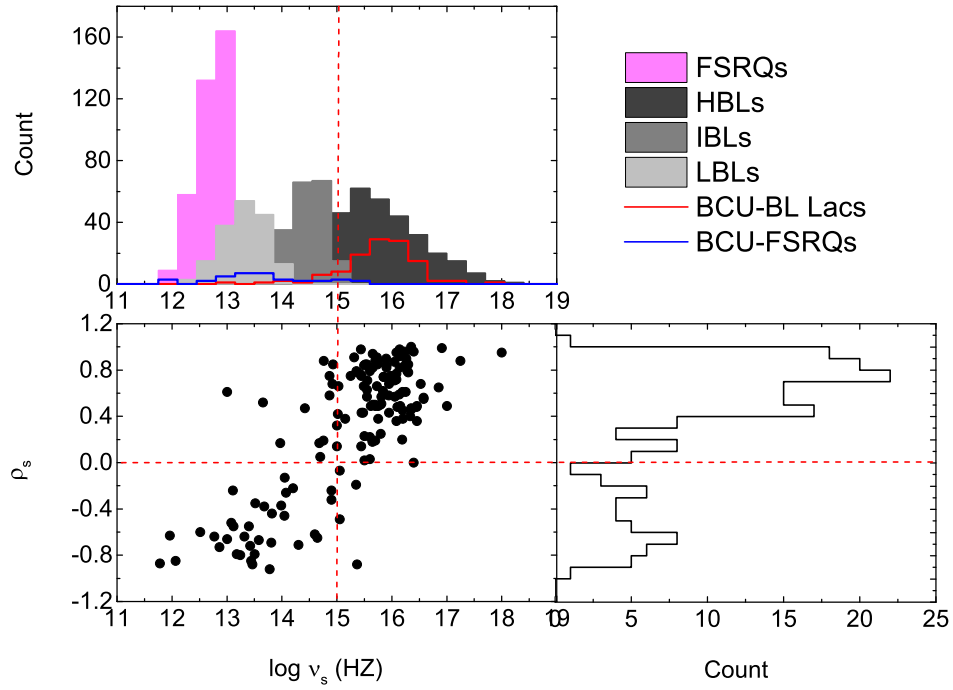


Fig. 5.— Distributions of the X-selected BCU sample in 1-dimensional and 2-dimensional planes of  $\rho_s$  and  $\log \nu_s$ . Comparisons of the  $\log \nu_s$  distributions for BL Lac candidates and FSRQ candidates picked up with our method to different sub-classes of FSRQs and BL Lacs from the reference sample are also shown in the upper panel.

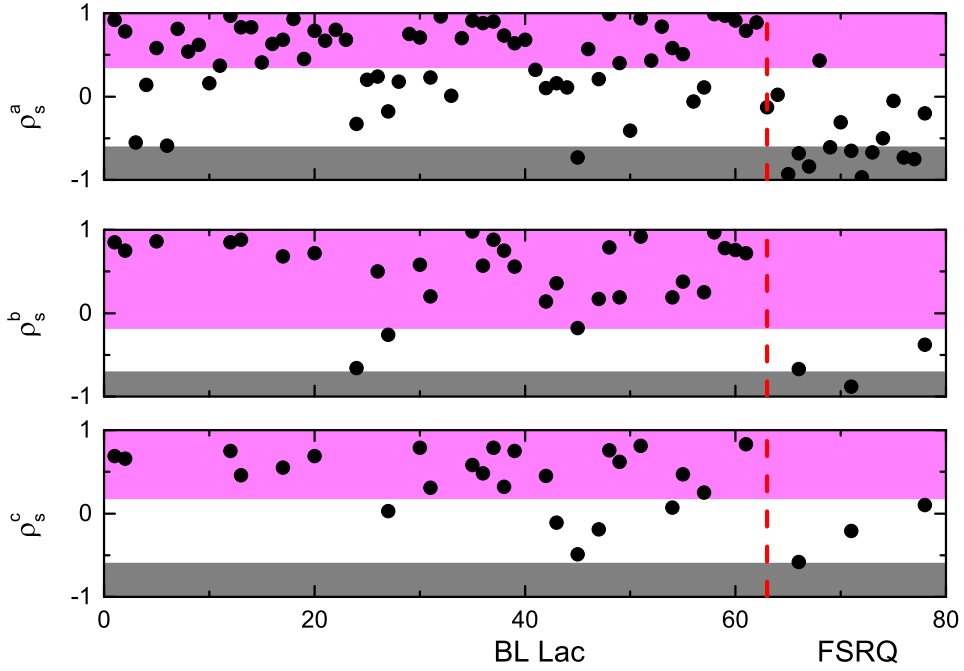


Fig. 6.— Examination of the consistency of our results with spectroscopic identification case by case using a sample taken from Massaro et al. (2016). X-axis marks the source number only, and the vertical dashed line separates the BL Lacs and FSRQs that are optically identified by Massaro et al. (2016, reference therein).  $\rho_s^a$ ,  $\rho_s^b$ , and  $\rho_s^c$  shown in the Y-axis for each panel are for the radio, X-ray, optical selected sources, respectively. The pink (BL Lac-like) and grey (FSRQ-like) regions mark the type evaluations with our method within  $\sigma > 90\%$ .